Iron Isotope Systematics in Estuaries: The case of North River, Massachusetts (USA)

Raphaelle Escoube[1,2], Olivier J. Rouxel[1*], Edward Sholkovitz[1] and Olivier F.X. Donard[2]

1. Marine Chemistry & Geochemistry Dept., Woods Hole Oceanographic Institution, Woods Hole, MA02543, USA
2. LCABIE, U. Pau et Pays de l'Adour, CNRS UMR 525, Hélioparc 64053 Pau, France

* *Corresponding author:* orouxel@whoi.edu

Geochimica et Cosmochimica Acta

Abstract:

Recent studies have suggested that rivers may present an isotopically light Fe source to the oceans. Since the input of dissolved iron from river water is generally controlled by flocculation processes that occur during estuarine mixing, it is important to investigate potential fractionation of Fe-isotopes during this process. In this study, we investigate the influence of the flocculation of Fe-rich colloids on the iron isotope composition of pristine estuarine waters and suspended particles. The samples were collected along a salinity gradient from the fresh water to the ocean in the North River estuary (MA, USA). Estuarine samples were filtered at 0.22 μm and the iron isotope composition of the two fractions (dissolved and particles) were analyzed using high-resolution MC-ICP-MS after chemical purification. Dissolved iron results show positive δ^{56}Fe values (with an average of 0.43 ± 0.04 ‰) relative to the IRMM-14 standard and do not display any relationships with salinity or with percentage of colloid flocculation. The iron isotopic composition of the particles suspended in fresh water is characterized by more negative δ^{56}Fe values than for dissolved Fe and correlate with the percentage of Fe flocculation. Particulate δ^{56}Fe values vary from -0.09‰ at no flocculation to ~ 0.1‰ at the flocculation maximum, which reflect mixing effects between river-borne particles, lithogenic particles derived from coastal seawaters and newly precipitated colloids. Since the process of flocculation produces minimal Fe-isotope fractionation in the dissolved Fe pool, we suggest that the pristine iron isotope composition of fresh water is preserved during estuarine mixing and that the value of the global riverine source into the ocean can be identified from the fresh water values. However, this study also suggests that δ^{56}Fe composition of rivers can also be characterized by more positive δ^{56}Fe values (up to 0.3 per mil) relative to the crust than previously reported. In order to improve our current understanding of the oceanic iron isotope cycling, further work is now required to determine the processes controlling the fractionation of Fe isotopes during continental run-off.

Keywords: *iron isotopes, rivers, estuary, flocculation, iron cycle, colloids*

1. Introduction

Although iron (Fe) is the 4th most abundant element in the Earth's crust (Taylor et al., 1983; Wedepohl, 1995), its concentration decreases to trace levels (< 1 nM) in the ocean (Wu et al., 2001; Boyle et al., 2005; Johnson et al., 1997). Because Fe acts as an essential micronutrient in biological processes (e.g. phytoplankton growth), iron concentration in the ocean is considered to be a limiting factor for primary productivity in large regions of the open ocean (Martin, 1990; Lefevre and Watson, 1999; Archer and Johnson, 2000; Boyd et al., 2000; Christian et al., 2002; Moore et al., 2002; Moore et al., 2004). The main sources of dissolved Fe into the ocean are wet and dry deposition from the atmosphere, input from rivers, re-suspended sediment, pore water from continental shelves and hydrothermal vents (e.g. Wells et al., 1995; Elderfield and Schultz, 1996; Johnson et al., 1999; Elrod et al., 2004; Jickells et al., 2005; Bennett et al., 2008).

Iron isotopes exhibit natural δ^{56}Fe variations of ~5‰ (Anbar, 2003; Beard and Johnson, 2004; Dauphas and Rouxel, 2006; Johnson and Beard, 2006) and provide potential new approaches to constrain the relative contribution of Fe sources in the oceans, and to improve our understanding of how Fe is mobilized from source regions (i.e. rivers, sediments) and transported into the ocean. In practice, the Fe isotopic composition of the various sources to the oceans is not well documented but recent studies have suggested that major sources of iron provide significant inputs of low- δ^{56}Fe iron to the oceans. In fact, continental run-off (Fantle and De Paolo, 2004; Bergquist and Boyle, 2006), hydrothermal sources (Beard et al., 2003a; Rouxel et al., 2008a), diagenetic pore fluids from shelf sediments and subterranean estuaries (Severmann et al., 2006; Rouxel et al., 2008b) have been suggested as potential negative δ^{56}Fe sources in seawater. The focus of this paper will be on the river and estuarine component of the iron geochemical cycle. We present a comprehensive study of the variation in Fe isotope composition of dissolved and particulate iron across the river/ocean mixing zone.

Large scale removal of river-borne dissolved Fe is a common feature of estuaries. Hence, the river input of dissolved Fe into the ocean is greatly modified by the salt-induced flocculation of Fe-humic-colloids that occurs during the mixing of fresh water and seawater (Eckert and Sholkovitz, 1976; Sholkovitz, 1976, 1978; Boyle et al., 1977; Mayer, 1982; Hunter, 1990).

84 The estuarine reactivity of the river-borne colloids depends on the speciation of iron, a
85 factor which may also control Fe-isotope composition (e.g. Brantley et al., 2001; Brantley
86 et al., 2004; Johnson et al., 2004). In a preliminary study, Bergquist and Boyle (2006)
87 reported the Fe-isotope composition of colloids precipitated during river water–seawater
88 mixing experiments using the Solimões River water. Although the isotopic shifts in the
89 flocculent (+0.2‰) was small and close to the analytical uncertainty, those results imply
90 that the remaining Fe in solution may be isotopically lighter than the Fe in the river water
91 end-member. Hence, it is presently unknown whether flocculation processes in natural
92 estuarine systems can significantly affect the iron isotope composition of riverine
93 discharged Fe to seawater.
94 The first aim of this paper is to determine if the large scale removal of dissolved Fe
95 during estuarine mixing will affect the iron isotope values of estuarine waters. Since
96 estuaries act like a "filter" for terrestrially-derived dissolved iron, it is important to test
97 whether this "filter effect" modifies the isotopic value of river-borne Fe within the
98 estuaries mixing zone. Our second objective is to characterize the Fe-isotope systematics
99 between dissolved and particulate pools in estuaries and to assess the impact of rivers on
100 the Fe-isotope composition of seawater. To this end, a series of model equations will be
101 developed and applied to a set of dissolved and particulate samples from the North River
102 estuary.
103
104 **2. Material and location**
105 We collected water and suspended particles along the North River Estuary
106 (Massachusetts, USA) in October 2006 (**Fig.1**). This river was chosen because of its high
107 concentration of dissolved organic matter and colloidal iron, its proximity and convenient
108 access as well as its limited urbanization setting. The waters of the North River and its
109 estuary are distinctly yellow-brown in color due to dissolved humic substances. Typically,
110 this type of river contains dissolved Fe in the form of colloids (Sholkovitz, 1976; Ross
111 and Sherrell, 1999). The estuary watershed extends over 85 km^2 and is primarily
112 composed of salt marshes with Paleozoic and Precambrian igneous and metasedimentary
113 rocks. The estuary can be physically characterized as partially mixed to vertically
114 homogeneous. As such, the surface water salinity changes gradually along the narrow
115 channel of the estuary; this allowed us to collect samples with small (0.2 PSU) differences
116 in salinity (**Fig.1**).

A 13' fiberglass boat was used to collect water samples at high and low tide in October 2006 (NR1, **Table 1**). Samples were collected in the central part of the river and estuary by attaching acid-washed 1L polyethylene (LPDE) bottles to a 2 m long plastic pole and dipping the bottle to a depth of 30 cm depth. Salinity and temperature were measured on site using an onboard YSI® probe. Salinity data are presented in Table 1. During the sampling time, water temperature was restricted between 13.5 and 12°C. One month later, a second set of freshwater samples (NR2) was collected from the North River in the town of Hanover, MA at the Elm St park at approximately 2 km up stream of the NR1 sample. This upstream site never experiences the intrusion of salt water and then represents fresh water background. The NR2 samples were collected to obtain more isotopic data for the fresh water end-member; these samples were also used for more complex types of filtration procedures.

Two samples of river water from the Connecticut River and Mullica River were also analyzed for the Fe-isotope composition of their dissolved Fe pool. The Connecticut River drains a large region of northeast North America and is the largest river entering the ocean in New England (Garvine, 1975). Like the North River, the Mullica River (New Jersey, USA) contains high concentrations of humic-type organic matter and colloidal Fe (Yan et al., 1990; Ross and Sherrell, 1999). Humic substances impart a dark yellow-brown color to the river water.

3. Analytical method

3.1. Sample filtration

We operationally define "dissolved iron" as the Fe that passed through a 0.22 μm filter. This < 0.22 μm fraction contains colloidal and truly dissolved (i.e. soluble) Fe pools. Although not measured, the soluble Fe pool is operationally defined as a non-colloidal fraction that is not affected by flocculation process in the estuary and is likely composed of organically bound iron. The particulate fraction consists of particles retained by 0.22 μm filters; this > 0.22 μm fraction contains the suspended sediment as well as newly precipitated colloids in the estuary. Less than 8 hours after sample collection, the water samples from the North River estuary were pressure (using N_2 at 31 PSI) filtered through Durapore^{TM} membrane type filters manufactured by Millipore Corp.. The filters were 47 mm in diameter and had a nominal pore size of 0.22 μm. Polycarbonate plastic

filter holders by Sartorius Ltd. were acid cleaned and used for the pressure filtration step. Filtered water samples were acidified to pH ~ 2 using ultra-pure (Optima-grade) 1N HCl. For each sample, a non-acidified aliquot of 15 mL was kept for color measurement. The filters were stored dried.

One of the river water samples, collected upstream of the estuary in November 2006 (sample NR2), was pressure filtered as describe above. A second sample was handled differently; it was pumped through a Millipore Millipak^{TM} cartridge filter unit that contained 0.22 μm pore size Durapore^{TM} filter material. The water obtained from the pressure filtering method was then refiltered in parallel through 0.1, 0.05 and 0.025 μm membrane filters. This filtration scheme was designed to characterize the colloids within the dissolved pool (<0.22 μm) of Fe. The three fractions collected correspond to three size ranges of colloids: 0.22-0.1 μm; 0.22-0.05 μm and 0.22-0.025 μm.

The Mullica River water was filtered using a hand-held all-plastic syringe with a 0.22 μm pore size filter unit from Millipore. The water was filtered on a small boat on June 26th 2007 and acidified on the spot. The Connecticut River water was collected off a small boat, pressure filtered on May 22nd 2007 and acidified as described for the North River.

3.2. Chemical analysis

According to Sholkovitz (1976), the adsorption measurement of the UV-Vis spectra of unacidified filtered water samples at wavelengths of 350 nm and 465 nm provide an approximation of the humic acid content of the filtered samples. These measurements were carried out in a 5 cm quartz cell. Total dissolved iron concentrations of the acidified filtered water samples were measured by UV-Vis spectrophotometry using the Ferrozine method modified from Stookey (1970). A reductant (Hydroxylamine HCl) was used to obtain concentrations of total dissolved Fe. Measurements were performed at a wavelength of 562 nm in 5 cm quartz cell.

Multi-elemental analysis of the acidified filtered water and digests of the suspended particles were carried out on a ICP-MS (Finnigan Element 2). The filters were leached overnight with 6 mL of 7N distilled HNO_3 in 15 mL closed Teflon vials on a hot plate at 80°C. The solutions were then slowly evaporated to dryness. A second dissolution step using 0.5 mL of concentrated ultrapure HF and 2 mL of concentrated distilled HCl was then used to obtain a total digestion of the particles. 5 mL of distilled and

concentrated HNO_3 and 1 mL of H_2O_2 were added and the filters were removed before the solution was taken to dryness. The solid residue was dissolved in 10mL of 2% HNO_3 (Optima grade) and an aliquot was further diluted for multi elemental ICP-MS analyses. The remaining solution was saved for Fe-isotope analysis. Acidified water samples were diluted to 1:7 with 2% HNO_3 (Optima grade). Indium solution was added to a final concentration of 5 ppb to correct for ICP MS sensitivity changes due to matrix effects. Four multi element standards with a salinity of 0, 0.9, 1.4, and 3.3 respectively were analyzed as calibration points. Water analysis reported in **Table 1** includes Fe, Ca, Mo, Mn, Al while Ti, Cr, Co, Zn and Cu were below detection limit and are not reported. Particulate concentrations for Al, Fe, Ti, Ca and Mn are reported in Table 2.

3.3. Iron isotope analysis

A volume of not more than ~40 mL of estuarine water with a salinity < 15 was evaporated to dryness in Teflon vials with 1 mL of concentrated distilled HNO_3 to release the iron from organic complexes. The maximum operational volume for saline water reflects the high load of salts that prevent evaporating larger volume of waters without subsequent problems during chromatography separation. Consequently, Fe-isotope analysis were performed only for samples with <15 salinity. The acid solution was taken to dryness at 80°C on a hot plate. A subsequent evaporation was done with 10 mL of distilled 7N HNO_3 with 1 mL of H_2O_2 (ultrapure grade). For the particulate analysis, the solution obtained after complete digestion (section 3.1) was evaporated on a hot plate. For both river water and particle samples, the solid residue were dissolved with 4 mL of distilled 6N HCl and one drop of H_2O_2 to ensure the complete oxidation of Fe. This solution was loaded onto a chromatography column filled with 1.5mL (wet volume) of anion exchange resin (AG1-X8, Bio-rad) previously cleaned with 10 mL of 3N HNO_3 and 10 mL of 18mΩ H_2O. Prior to sample loading, the resin was conditioned with 5 mL of distilled 2% HCl followed by 2.5 mL of distilled 6N HCl. After loading the sample, 25 mL of distilled 6N HCl was passed through the resin to elute the matrix. Iron is then eluted with 12.5 mL of distilled 0.24N HCl and collected in 15 mL Teflon vials. Samples were evaporated to dryness on a hot plate at 80°C and dissolved with 3mL of distilled 0.24N HNO_3 ready for isotope analysis.

Fe isotope compositions were determined with a Finnigan *Neptune* multicollector inductively coupled plasma mass spectrometry (MC-ICPMS) at WHOI using the method described in Rouxel et al. (2005; 2008a). The *Neptune* instrument permits high precision

measurement of Fe isotope ratios without argon interferences using the high-mass resolution mode (Weyer and Schwieters, 2003; Poitrasson and Freydier, 2005). Mass resolution power of about 8000 (medium resolution mode) was used to resolve isobaric interferences, such as ArO on ^{56}Fe, ArOH on ^{57}Fe, and ArN on ^{54}Fe. Instrumental mass bias is corrected using Ni isotopes as internal standards. The method, which has proved to be reliable for the Neptune instrument, involves deriving the instrumental mass bias by simultaneously measuring ^{62}Ni/^{60}Ni isotope ratios.

Samples were generally introduced in the plasma torch using a quartz spray chamber equipped with Teflon nebulizer (50 µl/min). In some cases, increased instrument sensitivity was required and the analyses were performed using X-cones. Under these conditions, sample solutions were measured with concentrations ranging from 0.5 to 3 ppm. In all cases, the samples were diluted with 2% optima HNO_3 in appropriate concentrations so that the IRMM-014 bracketing standards had the same concentration as the sample. Potential ^{54}Cr interference was monitored by measuring ^{52}Cr intensity using peak jumping in medium resolution mode to avoid ^{40}Ar^{12}C interferences.

Because instrumental mass bias is sensitive to matrix effects, we measured Mg and Ca concentrations prior to isotope measurements. The aim is to quantify the efficiency of the purification scheme by measuring elements present in seawater matrix. In all cases, we verified that matrix elements were <1% of the total Fe concentration. Because Fe isotopes can be fractionated during column chromatography (Anbar et al., 2000), we also verified the yield of the purification step. For each sample, the matrix solution eluted from the anion-exchange resin was collected in Teflon vials, evaporated and then analyzed by spectrophotometry using the ferrozine method. In all cases, the loss of iron during the purification step is less than 1%.

All analyses are reported in delta notation relative to the IRMM-014 standard, expressed as δ^{56}Fe, which represents the deviation in per mil relative to the reference material:

$$\delta^{56}Fe(‰) = \left(\frac{(^{56}Fe/^{54}Fe)_{sample}}{(^{56}Fe/^{54}Fe)_{IRMM-014}} - 1 \right) \times 1000 \qquad (1)$$

We also reported δ^{57}Fe values but, since the relationships between δ^{56}Fe and δ^{57}Fe of the samples plot on a single mass fractionation line, only δ^{56}Fe values are discussed in this paper.

In order to check the accuracy of our Fe-isotope analyses in estuarine waters, natural seawater matrices were doped with IRMM-014 standard and processed through the complete chemistry steps as unknown samples. Duplicated purification and analysis gave an average of $\delta^{56}Fe$ = 0.01 ‰ (2 σ = 0.06 ‰) for 17 samples which compared well with pure standard processed through chemistry (in 18mΩ H_2O). The average Fe blank measured in seawater matrices processed through chemistry was 10 ng, which corresponds to about 0.1 % for the water samples and 0.01 % of the filters.

4. Results

4.1. River end-member composition

The river water end-member concentration of dissolved iron during the Oct. 2006 sampling of the estuary is 7.0 μM (**Table 1**). The sampling of the upstream river site on Nov. 2007 (sample NR2) yielded 8.7 and 8.8 μM of dissolved Fe using cartridge and membrane filtering methods (**Table 3**). The Mullica and Connecticut River yielded dissolved Fe concentrations of 8.3 μM and 1.4 μM respectively (**Table 4**). Hence, the two highly colored and organic-rich rivers contained significantly more dissolved Fe than the Connecticut River.

Filtering a North River water sample through 0.22, 0.1, 0.05 and 0.025 μm pore-size membranes lead to similar concentrations of Fe (8.8, 8.7, 8.3 and 8.7 μM respectively, **Table 3**). While our filtration scheme was designed to remove colloidal Fe from the river water sample, filtration down to a nominal pore size of 0.025 μm didn't remove colloidal Fe (**Table 3**). Likewise, the Fe retained by the 0.1 and 0.025 μm pore-sized filters was very low (0.08 μM) with respect to all four filtered fractions (~8.7 μM) and to the particle (> 0.22 μm) Fe fraction (3.17 μM). Hence, the Fe retained by 0.1 and 0.025 μm filters represents less than 1% of the total dissolved (<0.22 μm) Fe pool. Only the Fe retained between the 0.22 and 0.05 μm fractions contained a significantly amount of Fe (0.47 μM). Again, this Fe only represents 5% of the fraction of Fe passing through the four different filter sizes. Hence, both the filtered and retained Fe for the pore-size study show that filtration down to 0.025 μm was not small enough to remove colloidal Fe from the river water of the North River. As discussed in the next section, there is large (83%) removal of dissolved (<0.22 μm) Fe in the North River estuary. This removal is almost certainly due to the salting-out of river Fe colloids. Hence, the colloids removed during estuarine mixing must be smaller in size than 0.025 μm.

283

284 The isotopic Fe composition of three filtered (<0.22 μM) NR2 river water samples
285 displays positive δ^{56}Fe values of similar magnitude relative to IRMM-014 standard.
286 These values are 0.37, 0.34 and 0.38‰ (**Tables 1 and 3**). These values are also ~0.3‰
287 heavier than the bulk Earth value defined at 0.09‰ relative to IRMM-14 (Beard et al.,
288 2003a; Dauphas and Rouxel, 2006). In contrast, the total particulate Fe fraction (>0.22
289 μm) of upstream river site had the most negative δ^{56}Fe value at -0.22‰ (**Table 3**). The
290 two lowest salinity samples of the estuarine transect also had negative δ^{56}Fe value at -0.09
291 and -0.01‰ Hence, the difference between dissolved and particulate Fe in North River is
292 about 0.5‰ (+ 0.37 vs. -0.1‰).

293 Iron passing through 0.22 μm to 0.025 μm filter pore size show negligible variations
294 in Fe-isotope compositions (average δ^{56}Fe of 0.39 ± 0.04‰). As noted above, these four
295 filtrates also show little variation in their dissolved Fe concentrations (~8.3-8.8 μM). The
296 Fe fractions retained by the 0.1, 0.05 and 0.025 μm pore-sized filters (starting with the
297 <0.22 μm filtrate) are characterized by a δ^{56}Fe composition of -0.12, 0.14 and 0.09 ‰
298 respectively. These 'colloidal" values are more positive than the river (>0.22 μm)
299 particles at -0.22‰ but lower than all four filtrates (< 0.22 down to <0.025 μm) at 0.34 to
300 0.44 ‰ (**Table 3**). As noted above, our size-filtering scheme yields little in the way of
301 colloidal Fe. Hence, our pore-size study was not able to directly characterize the Fe
302 isotopic composition of the major pool of river colloids in the North River. Ultrafiltration
303 techniques are part of on-going project to isolate the pool of Fe colloids.

304

305 *4.2. Element behavior in North River estuary*

306 The estuarine distributions of dissolved (<0.22 μm) Fe and Al along the salinity
307 gradient of North River estuary show that both elements deviate markedly from
308 conservative mixing with very similar shapes (**Fig. 2**). The salinity distribution of
309 dissolved Fe and Al remain similar under ebb and flood tides conditions. Hence, we will
310 consider the two transects as one. This observation also permits us to assume that iron
311 precipitation is only salinity-dependant.

312 Large scale net removal of dissolved Fe during estuary mixing in the North River is a
313 common feature of estuaries (Boyle et al., 1977; Sholkovitz et al., 1978; Mayer, 1982;
314 Fox and Wofsy, 1983; Forsgren et al., 1996; Hunter et al., 1997; Gustafsson et al., 2000).
315 Though much less studied than Fe, field results confirm that the non-conservative removal

316 pattern of Al does occur in estuaries (Hydes and Liss, 1977; Crerar et al., 1981;
317 Upadhyay, 2008). Ultrafiltration studies (Ross and Sherrell, 1999) and laboratory-based
318 experiments (Eckert and Sholkovitz, 1976) also show that dissolved Al in organic rich
319 rivers exists as humic-type colloid and undergoes extensive salt-induced flocculation.
320
321 The percentage of Fe removal during estuarine mixing has been calculated following
322 the flux model of Boyle et al. (1974). The explicit formulation of this mixing model
323 implies that, over straight-line segments of the curve, simple two end-member dilution
324 processes can be considered. Using this approach, pure river and seawater end-members
325 as well as the percentage removal of Fe can be determined. Because the salinity along
326 North River estuary ranges from 0.2 to 30, we can extrapolate our measured dissolved Fe
327 concentrations at low salinity (i.e. S between 0.2 and 5) to derive the Fe concentration for
328 the river water end-member as 7.5μM. Similarly, we can extrapolate our measured
329 dissolved Fe concentrations at high salinity (i.e. S between 20 and 30) to derive the Fe
330 concentration at the zero-salinity intercept as 1.4μM (**Table 4**). The removal of Fe due to
331 the flocculation process is then estimated by the difference between the initial Fe
332 concentration in the river end-member and the Fe concentration at the zero-salinity
333 intercept. The model results yield a net removal of 83% for dissolved Fe in North River
334 estuary; this value compares well with other estuaries in the northeast United States
335 (Boyle et al., 1977). The net removal for dissolved Al is also large ~ 85%. Color can
336 serve as a semi-quantitative proxy of dissolved humic substances (Eckert and Sholkovitz,
337 1976; Sholkovitz, 1976). **Figure 2** shows there is small, but significant, amount of
338 removal of dissolved humic compounds (i.e. color) from the river water during estuarine
339 mixing. The color removal, based on the salinity distribution model of Boyle et al. (1974)
340 is ~ 30%. As expected, the results show a linear relationship between Ca and Mo with
341 salinity, consistent with conservative behavior during estuarine mixing.
342 The distribution of particulate Fe concentration vs. salinity is presented in **Figure 3**
343 and display a sharp decrease at low salinity, from 7 μM in the river end-member down to
344 3 μM at salinity of 5. The ratio of dissolved Fe relative to particulate Fe (**Figure 3**)
345 indicates that approximately 45 to 50% of the total Fe in North River is carried in the
346 dissolved load. This proportion decreases to less than 5% at the high-salinity end of the
347 estuary.
348

349 *4.3. Determination of the flocculation factor*

350 In order to relate potential Fe-isotope fractionation during the flocculation process, we
351 calculated the fraction (*F*) of dissolved Fe removed in each sample along the salinity
352 gradient. *F* is calculated using the ratio of measured Fe concentration corrected from
353 seawater mixing, *versus* the initial dissolved Fe concentration in the river (i.e. freshwater)
354 end-member, such as:

355 $$F = 1 - \left(\frac{Fe_{SW}}{Fe_{RW}} + \frac{Fe_S - Fe_{SW}}{Fe_{RW}} \times \frac{1}{1 - S/35} \right) \quad (2)$$

356 Where Fe_{SW} is the concentration of Fe in the seawater end-member (less than 0.01
357 μM), Fe_s the measured concentration at the salinity S, and Fe_{RW} the concentration in the
358 river end-member (7.5 μM). Although the concentration of dissolved Fe in local coastal
359 seawater has not been determined, total dissolved Fe concentrations of about 10 nM have
360 been already reported in surface seawater of Massachusetts Bay by Zhuang et al. (1995).
361 Because end-member seawater Fe concentrations represent less than 1% of the initial Fe
362 from the river, using seawater Fe concentrations of up to 20nM, as found in other local
363 coastal seawater (Rouxel, 2009) has no effects on the value of F. As presented in **Figure**
364 **4**, the fraction of Fe removed by colloid flocculation shows a drastic increase up to 0.5
365 below a salinity of 5 then increases slowly up to 0.7 for a salinity of 10. At higher salinity,
366 the percentage of flocculated iron is relatively stable between 70 to 80%. The Fe-isotope
367 compositions of both particulate and dissolved Fe pools along the salinity gradient of
368 North River estuary are presented in **Table 2** and **Figure 5**. The dissolved Fe pool (i.e. <
369 0.22 μm fraction) does not display any systematic changes in δ^{56}Fe values along the
370 estuary and yields an average Fe-isotope composition of 0.43 ± 0.04‰. In contrast,
371 particulate Fe-isotope compositions increase from -0.1 to 0.15‰ between salinities of 0.2
372 to ~5‰. At higher salinities, suspended particles yield δ^{56}Fe values similar, within
373 uncertainties, to crustal materials defined at 0.09‰ (Rouxel et al., 2003; Beard et al.,
374 2003a,b).
375
376 **5. Discussion**
377
378 *5.1. Fe-isotope systematics in colloidal and particulate pools in the river end member*

379 An important result of this study is that the dissolved Fe fraction of North River
380 has a positive δ^{56}Fe value of ~0.4‰ which is heavier than the crustal composition defined

381 at ~0.09‰ and heavier than most previous studies in other riverine systems (Fantle and
382 DePaolo, 2004; Bergquist and Boyle, 2006; Ingri et al., 2006). Another important result is
383 the significant differences in Fe-isotope compositions between the dissolved and
384 particulate iron in the riverine end-member. This difference reaches 0.46‰ and 0.60‰ in
385 North River sampled in October and November 2006 respectively.
386 Although Fantle and DePaolo (2004) analyzed unfiltered river water, they
387 proposed that soluble Fe in rivers is characterized by more negative δ^{56}Fe values
388 compared to the average crust (i.e. δ^{56}Fe values between -0.78 to 0.13‰ for 8 rivers from
389 North America). Bergquist and Boyle (2006) reported δ^{56}Fe composition of filtered (<0.4
390 μm) Amazon River waters showing negative value (from -0.46 to -0.08‰) while the
391 Negro River water displayed heavier Fe-isotope composition (from 0.2 to 0.44‰). In
392 another study of Fe-isotope composition of suspended matter in a Boreal river in Sweden,
393 Ingri et al., (2006) proposed that Fe (III) – humic acid complexes represent a light pool of
394 iron isotopes in river colloids while Fe hydroxides would yield higher δ^{56}Fe values.
395 Altogether, with the exception of the Rio Negro, most previous studies are consistent with
396 the preferential loss of light Fe-isotopes during weathering and mineral dissolution
397 processes (Brantley et al., 2004; Thompson et al., 2007). However, the hypothesis that
398 organically-bound Fe in rivers can be characterized by lighter Fe-isotope composition is at
399 odd with the enrichment in heavy Fe isotopes in river colloids at North River. In
400 particular, the Fe-isotope analysis of various size fraction of colloids at North River
401 (**Table 3**) suggests that the larger colloidal fraction (e.g. >0.025 μm) are lighter by up to
402 0.3‰ relative to finer colloids (e.g. <0.025 μm). Hence, these results confirm that
403 colloids, probably composed of Fe(III)-humic or other organic ligand complexes, yield
404 positive δ^{56}Fe values relative to suspended sediments.
405 The Connecticut and Mullica rivers yielded δ^{56}Fe values of 0.18 ‰ and -0.33 ‰
406 respectively. This large variation between these two rivers suggest that the value of iron
407 isotope is not principally controlled by the organic content in the water: the Connecticut
408 River, which represents a large mineral discharge of North East America, has lower
409 content of dissolved humic compounds than North River but has slightly lower δ^{56}Fe
410 values. Hence, the high value δ^{56}Fe for North River is at odds with the expectation that
411 Fe-C compounds are characterized by lighter Fe-isotope composition. Only Mullica
412 River, which is characterized by the highest organic matter content and Fe concentration
413 (Sholkovitz, 1976; Crerar et al., 1981; Yan et al., 1990) is characterized by lower δ^{56}Fe

414 values than crustal material may be consistent with the preferential partitioning of light
415 Fe-isotopes with organic compounds.
416 In principle, Fe isotopes variability in rivers can be related to the mineralogy of the
417 rocks and sediments present in watersheds, the weathering regime (chemical vs. physical
418 erosion), and the presence of ligands during weathering (Brantley et al., 2004; Fantle and
419 DePaolo, 2004). In addition, changes in iron isotopes composition can also be linked to
420 biological (Johnson et al., 2004) and chemical processes such as adsorption (Icopini et al.,
421 2004; Teutsch et al., 2005), precipitation (Skulan et al., 2002), and redox conditions
422 (Severmann et al., 2006; Rouxel et al., 2008b).
423 Although the Fe isotope composition of the upper continental crust has been
424 recently debated in the literature (Poitrasson and Freydier, 2005; Beard and Johnson,
425 2006; Poitrasson, 2006), numerous evidences suggest that sedimentary clastic rocks have
426 average δ^{56}Fe value similar to igneous rocks. Only a limited number of high-SiO_2 granitic
427 rocks (δ^{56}Fe up to 0.4‰) have been shown to deviate from the igneous average. However,
428 those crustal components have likely a minimal impact on the global composition of the
429 continental crust. Hence, it is unlikely that the high- δ^{56}Fe values of dissolved Fe observed
430 at North River is due to the weathering of isotopically heavy rocks.
431 Among other processes, the precipitation or adsorption of isotopically light Fe
432 onto riverine particles may also explain positive δ^{56}Fe values in the dissolved pool. The
433 observation that suspended particulate matter in North River has δ^{56}Fe values ~0.5‰
434 lower than the dissolved pool is consistent with this hypothesis. Similar to North River,
435 the Negro River in the Amazon system, which displays heavier Fe-isotope composition
436 (up to 0.44‰) for dissolved Fe, has particulates up to ~ 1.2 ‰ lighter than the associated
437 dissolved Fe. We also note that similar results have been already reported for other
438 isotope systems such as Li (Huh et al, 2001) and Cu (Vance et al, 2008) isotopes. In
439 particular, heavier Cu-isotope compositions of the dissolved phase relative to the
440 particulate Cu-pool have been interpreted as resulting from an equilibrium isotope effects.
441 The process of Fe-isotope fractionation between dissolved and particulate pools remains,
442 however, unclear as the nature of Fe-species involved is unknown. Approximately half of
443 the total Fe in North River is carried in the dissolved load (**Figure 3**). Hence, the δ^{56}Fe
444 value for total Fe is ~ 0.1‰ which is similar to the bulk crust value. This suggests that the
445 total Fe-isotope composition in the riverine system is not significantly fractionated by
446 continental run-off but that the production of colloidal organic species may produce

447 significant Fe-isotope fractionation between particulate and colloidal pools. Recent
448 experimental studies of isotope fractionation between organically bound and inorganic
449 Fe(III) species in solution are consistent with this hypothesis. Dideriksen et al., (2008)
450 found that Fe(III) bound to strongly coordinating ligands is likely to yield heavier δ^{56}Fe
451 values (up to 0.6‰) than the inorganically complexed Fe, which may be removed from
452 solution through precipitation. In the case of North River, similar isotope effects may
453 occur: the preferential removal of isotopically light inorganic dissolved Fe (e.g. Fe-oxide
454 and clays) may leave the dissolved - organically complexed – colloidal pool enriched in
455 heavy isotopes. Alternatively, in the North River estuary, high concentration of dissolved
456 humic substances may provide stronger bonding environments than Fe-hydroxide- or
457 clay-rich particules. In this case, heavier Fe-isotope composition in the dissolved Fe pool
458 may result from direct Fe-isotope fractionation between dissolved and particulate pools,
459 whereby heavy isotopes are partitioned preferentially in the stronger bonding
460 environments (Urey, 1947 and Schauble, 2004), as recently observed for Cu-isotopes
461 (Vance et al, 2006). Additional studies of Fe-speciation in rivers (e.g. Gledhill and Van
462 den Berg, 1995) combined with Fe-isotope composition may solve this issue.
463 An alternate hypothesis is that the heavy δ^{56}Fe values in rivers are generated during the
464 preferential retention of light Fe-isotopes in soils, either through secondary mineral
465 precipitation (e.g. Wiederhold et al., 2007) or plant uptake (Guelke and Von
466 Blanckenburg, 2007). The fact that both dissolved and particulate pools in the North River
467 has Al/Fe ratios lower than crustal values (Al/Fe~0.15 vs Al/Fe~1.5, **Figure 6**) is
468 consistent with incongruent weathering and formation of (Fe,Al)-silicates in soils.
469 However, it is presently unclear if the Fe-isotopic difference between dissolved and
470 particulate phases may be influenced by weathering intensity as previously reported for Li
471 isotopic system (Huh et al, 2001).
472
473 *5.2. Fe-isotope systematics of dissolved Fe during flocculation process in estuaries*
474 Dissolved Fe has long been recognized as having a non-conservative behavior in most
475 estuaries (Boyle et al., 1977; Sholkovitz et al., 1978; Bale and Morris, 1981; Mayer, 1982;
476 Fox and Wofsy, 1983; Forsgren et al., 1996; Hunter et al., 1997; Gustafsson et al., 2000).
477 It is generally assumed that the coagulation of Fe-rich colloids results from the
478 destabilization of organic complexes and negatively charged-Fe colloids by seawater
479 cations. In this study, we have shown that most dissolved Fe in North River is affected by
480 large-scale removal at low salinity (<15‰), reducing the effective input of dissolved Fe to

481 the ocean by about 83% of the primary river value. The precipitation of organic-rich
482 riverine colloids at North River is also confirmed by the non-conservative behavior of
483 humic compounds (i.e. color) distribution along the estuary and by the removal of Al
484 (**Figure 3**), which is also closely associated with organic material (Eckert and Sholkovitz,
485 1976). Since the coagulation of Fe-humic colloids involves complex transformations
486 between labile, colloidal and particulate phases, estuaries may modify the isotopic
487 composition of riverine source of Fe to the oceans in the following cases:

488 (1) If chemical weathering results in river water having humic-Fe colloids with a
489 different isotopic composition than soluble Fe, then estuarine flocculation should lead to
490 modification of Fe isotope composition of dissolved Fe, reflecting the preferential
491 removal of colloids relative to labile Fe which are not affected by flocculation. At North
492 River, soluble Fe (i.e. pool of dissolved Fe which is not affected by flocculation process)
493 represents about 20% of the total dissolved Fe concentration, **Table 4**. The evolution of
494 dissolved δ^{56}Fe values relative to the amount *F* of Fe precipitated can be described by the
495 mass balance equation:

496 $$(1-F)\times\delta^{56}Fe = (F_{\max} - F)\times\delta^{56}Fe_{col} + (1-F_{\max})\times\delta^{56}Fe_{sol} \qquad (3)$$

497 Where F_{max} is the maximum extent of Fe precipitation in the estuary (determined at 0.83),
498 $\delta^{56}Fe_{col}$ and $\delta^{56}Fe_{sol}$ are the Fe-isotope composition of colloidal and soluble Fe end-
499 members. Note that this model does not include the potential contribution of seawater-
500 derived Fe which is estimated to be less than 0.01 μM, and thus negligible relative to river
501 borne Fe, even at the maximum salinity in North River estuary. Based on the relationship
502 between δ^{56}Fe and 1/(1-F) presented in **Figure 7**, the δ^{56}Fe difference between colloidal
503 Fe and labile Fe (calculated at F=0.9) is restricted to less than 0.14‰ ±0.15 (2SE) and
504 thus insignificant compared to the uncertainty (i.e. after error propagation).

505 (2) If significant Fe isotope fractionation occurs between particulate and dissolved
506 Fe, then estuarine mixing should lead to isotope fractionation during Fe removal. Because
507 colloids offer a much greater number of surface complexation sites than suspended
508 particles, potential exist for isotope fractionation during adsorption processes or during
509 precipitation/aggregation of colloids onto suspended particles. In this case, the
510 precipitation of humic-Fe colloids corresponds to a unidirectional process (i.e. no further
511 reactions between dissolved and particulate Fe pools), the fraction *F* of Fe precipitated, as
512 defined in equation (2), and the Fe-isotope composition in the remaining dissolve pool
513 can be determined by the Rayleigh law:

514 $$\delta^{56}Fe = (1000 + \delta^{56}Fe_0) \times (1 - F)^{(\alpha - 1)} - 1000 \quad (4)$$

515 where $\delta^{56}Fe_0$ is the initial value of the river end-member and α is the particulate-dissolved
516 fractionation factor during the flocculation process. Using this relationship, it is possible
517 to calculate the maximum α values producing the distribution of $\delta^{56}Fe$ values along the
518 estuary (**Figure 7**). Since $\delta^{56}Fe$ values of the estuarine samples are identical within
519 uncertainties, α equal to 0.99993 ± 0.00006 (2SE) which implies that Fe-isotope
520 fractionation during the flocculation processes is less than 0.07‰ and does not
521 significantly affect the iron isotopes of rivers within uncertainty.
522
523 *5.3. Fe-isotope systematics in the particulate pool*
524 Iron in suspended particles (>0.22 μm) is essentially associated with clays, humic
525 compounds and Fe oxides (e.g. Ross and Sherrell, 1999; Poulton and Raiswell, 2002;
526 Allard et al., 2004). In estuaries, newly formed particles due to colloid flocculation are
527 expected to represent another important pool of Fe. Although suspended particles in North
528 River are characterized by sub-crustal $\delta^{56}Fe$ values around -0.1‰, the precipitation of
529 isotopically heavy colloids should result in significant alteration (i.e. increase) of $\delta^{56}Fe$
530 values of estuarine particles. As illustrated in **Figure 2 and 6**, dissolved Al behaves
531 similarly to Fe in the estuary (i.e. non-conservative behavior) with Al/Fe being constant
532 over a wide range of salinity. In contrast, Al/Fe ratios in suspended particles display a
533 gradual increase with salinity, from dissolved Al/Fe ratios of ~ 0.15 (g/g) in the
534 freshwater end-member to sub-crustal values ~ 1.6 (g/g) at high salinity. Consequently,
535 particulate Al/Fe ratios cannot be explained by a simple binary mixing between river-
536 borne particles and newly formed particles due to colloid flocculation. A third Fe
537 component needs to be taken in consideration, that is, lithogenic particles with near
538 crustal Al/Fe ratios. This last source corresponds to a major part of suspended marine
539 sediments with an assumed Al/Fe ratios of ~ 2.0 (g/g) and crustal $\delta^{56}Fe$ (=0.09 ‰)
540 consistent with upper continental crust values (Dauphas and Rouxel, 2006; Rudnick and
541 Gao, 2007).
542 From the relationship between $\delta^{56}Fe$ and Al/Fe values in estuarine particles
543 (**Figure 8**), we can define 3-component mixing relationships such as:

544 $$\delta^{56}Fe_{part} = X_{RP} \times \delta^{56}Fe_{RP} + X_{Col} \times \delta^{56}Fe_{Col} + X_{Lith} \times \delta^{56}Fe_{Lith} \quad (5)$$

545 $$(Al/Fe)_{part} = X_{RP} \times (Al/Fe)_{RP} + X_{Col} \times (Al/Fe)_{Col} + X_{Lith} \times (Al/Fe)_{Lith} \quad (6)$$

where X_{RP}, X_{Col} and X_{Lith} correspond to the fraction of Fe in estuarine particles (*part*) derived from river-borne particles (*RP*), flocculated colloids (*Col*) and lithogenic particles (*Lith*) respectively. These values can be determined for each estuarine sample using the equations (5-6) which can be simplified considering that Al/Fe ratios in river-borne particles and colloids are similar, such as:

$$X_{Lith} = \left[(Al/Fe)_{part} - (Al/Fe)_{RP}\right] / \left[(Al/Fe)_{Lith} - (Al/Fe)_{RP}\right] \quad (7)$$

$$X_{Col} = \frac{\delta^{56}Fe_{RP} - \delta^{56}Fe_{part}}{\delta^{56}Fe_{RP} - \delta^{56}Fe_{Col}} - X_{Lith}\frac{\delta^{56}Fe_{RP} - \delta^{56}Fe_{Lith}}{\delta^{56}Fe_{RP} - \delta^{56}Fe_{Col}} \quad (8)$$

$$X_{RP} = 1 - X_{Col} - X_{Lith} \quad (9)$$

The mixing relationships between these three components are illustrated in **Figure 8a** showing δ^{56}Fe *vs.* Al/Fe ratios of dissolved Fe (<0.22 μm) and particulate Fe (>0.22 μm) along the North River estuary. The most striking feature is the increase of X_{Lith} with increasing salinity (**Figure 8b**). This suggests that lithogenic particles derived from local seawater end-member, probably through sediment resuspension along the coastal zone. In particular, the high-energy environments provided by coastal seawaters may carry significant suspended sediments that can mix with estuary particles. Although an increase of X_{Col} is observed at low salinity (S<5) due to flocculation process as river water mixes with seawater, the decrease of X_{Col} at higher salinity is more surprising. As mentioned previously, the Al/Fe ratios in suspended particles (i.e. X_{Lith}) display a gradual increase with salinity which result in relative decrease of riverine particles and colloids in the estuary. In **Figure 9**, the relationship between X_{Col}/X_{RP} and the flocculation factor (*F*) reveals a positive correlation with a slope close to unity (0.9 ± 0.1). As illustrated in **Figure 3**, approximately 45 to 50% of the total Fe in North River is carried in the dissolved load. Hence, the total fraction of colloidal Fe relative to river-borne particulate Fe, will be about 0.8 to 0.95 after quantitative flocculation (i.e. F=1). Hence, both independent approaches are in good agreement which confirms that only river-seawater mixing process and colloid flocculation control dissolve and particulate Fe concentration in North River estuary. In contrast, such processes have essentially no effect of Fe-isotope composition of dissolved Fe.

5.4. Implication for coastal seawater Fe sources

Among important sources of iron in coastal seawater, diagenetic pore fluids from shelf sediments (Staubwasser et al., 2006; Bergquist et Boyle, 2006; Severmann et al., 2006; 2008) and groundwater (Rouxel et al., 2008b) have been suggested to provide significant source of low- δ^{56}Fe iron to the oceans. Based on the observed homogeneity of Fe isotope composition of suspended loads of major rivers across the United States, it has been initially suggested that Fe inputs to the ocean via rivers is similar to igneous rocks (Beard et al., 2003b). However, later studies have suggested that continental run-off may represent another source of low- δ^{56}Fe iron in coastal waters (Bergquist and Boyle, 2006; Fantle and De Paolo, 2004; Ingri et al, 2006). Suspended load may have also δ^{56}Fe values fractionated towards negative values suggesting that Fe isotope composition of river-borne particles is not unique (Bergquist and Boyle, 2006, this study). Since the process of flocculation produces minimal Fe-isotope fractionation in the dissolved Fe pool, we suggest that the Fe isotope composition of dissolved Fe in rivers is preserved during estuarine mixing and that the global riverine source into the ocean can display both heavier and lighter δ^{56}Fe values (between -0.5 to up to 0.3 per mil) relative to the continental crust. Since different river types may have different colloid size and compositions that may behave differently than the North River, the total range of Fe-isotope composition of the worldwide rivers is still poorly known.

Despite those uncertainties, our study suggests that dissolved riverine Fe can be characterized by near crustal or slightly positive δ^{56}Fe values which contrast strongly with benthic Fe sources having strongly negative δ^{56}Fe values due to suboxic Fe cycling (Severmann et al., 2006; Rouxel et al., 2008b). Hence, Fe-isotopes can provide valuable tracers to distinguish various Fe-sources in coastal oceans and their potential impact in marine ecosystems. This hypothesis is consistent with a recent study of the 100 km long Scheldt estuary (de Jong et al., 2007) where negative δ^{56}Fe values down to −1.2‰ have been observed along a salinity gradient. The occurrence of low δ^{56}Fe values for dissolved Fe in the Scheldt estuary has been attributed to either Fe-isotope fractionation processes due to redox cycling in the estuary or from adsorption/precipitation of dissolved Fe onto particulate matter. Based on our study, it can be suggested that low δ^{56}Fe values in the Scheldt estuary result from the contribution of an additional Fe source, probably derived from the diffusive input of isotopically light Fe from anoxic estuary sediments. The potential addition of groundwater-derived Fe may also produce such negative Fe-isotope signature, as already observed in Waquoit Bay (Rouxel et al., 2008b; Rouxel 2009).

6. Conclusion

The major objective of this study was to determine the processes controlling the fractionation of Fe isotopes between continental run-off and the oceans. The main findings are:

(1) Continental run-off yields colloidal Fe pools in rivers that are isotopically distinct from particulate Fe pools. In particular, we demonstrated that the particulate and dissolved fractions in a small river in North Eastern US are characterized by a difference of Fe–isotopic composition of up to 0.5‰ which is almost 10 times the analytical uncertainty. The particulate fraction (>0.22 μm) yields negative δ^{56}Fe values while the dissolved fraction <0.22 μm yielded positive δ^{56}Fe values relative to the bulk continental crust.

(2) The large scale removal of river-borne dissolved Fe, a universal feature of estuaries, does not significantly modify the Fe isotopic signature of terrestrial dissolved Fe reaching coastal waters. This suggests that, although Fe has a distinctly non-conservative behavior in estuaries, the δ^{56}Fe composition of rivers is not modified in estuaries. Based on Al/Fe and Fe-isotope ratios, we also determined that the suspended pool along the North River estuary is controlled by the relative proportion of river-borne particles, coagulated river colloids and detrital Fe derived from coastal area.

These results contrast with previous finding suggesting mostly negative δ^{56}Fe values for dissolved Fe in rivers (Fantle and DePaolo, 2004; Bergquist and Boyle, 2006). The oceanic input of Fe from rivers could have a local influence on the iron composition of the costal ocean which can be distinguished from diagenetic input from marine sediment and groundwater, the later having essentially negative δ^{56}Fe values (Severmann et al., 2006; Rouxel et al., 2008b). Hence, Fe-isotopes provide valuable tracers of Fe-sources in hydrologic and marine environments. Additional work is now required to assess the importance of weathering regime and climate on the temporal and spatial variability of Fe isotope composition of rivers.

Acknowledgements

This study was supported by the National Science Foundation (OCE 0550066) to O. Rouxel and Edward Sholkovitz. Lary Ball, Jurek Blustajn, Paul B. Henderson, Rose Petrecca, Mar Nieto-Cid and Maureen Auro are thanked for there technical support. We thank Sébastien Bertrand, Carl Lamborg and Valier Galy for helpful comments on the manuscript. This work benefited from constructive reviews of AE C. Johnson, D. Borrok, S. Severmann and one anonymous reviewer. A special thank is addressed to J. Carlioz.

References

Allard, T., Menguy, N., Salomon, J., Calligaro, T., Weber, T., Calas, G., and Benedetti, M. F., 2004. Revealing forms of iron in river-borne material from major tropical rivers of the Amazon Basin (Brazil). *Geochimica et Cosmochimica Acta* **68**, 3079-3094.

Anbar, A., 2003. Iron stable isotopes: beyond biosignatures. *Earth Planet. Sci. Lett.* **217**, 223-236.

Anbar, A. D., Roe, J. E., Barling, J., and Nealson, K. H., 2000. Nonbiological Fractionation of Iron Isotopes. *Science* **288**, 126-128.

Archer, D. E. and Johnson, K., 2000. A model of the iron cycle in the ocean. *Global Biogeochemical Cycles* **14**, 269-279.

Bale, A. J. and Morris, A. W., 1981. Laboratory simulation of chemical processes induced by estuarine mixing: the behavior of iron and phosphate in estuaries. *Estuarine Coastal Shelf Sci.* **13**, 1-10.

Beard, B. L. and Johnson, C. M., 2004. Fe isotope variations in the modern and ancient Earth and other planetary bodies. *Reviews in Mineralogy and Geochemistry* **55**, 319-357.

Beard, B. L. and Johnson, C. M., 2006. Comment on "Heavy iron isotope composition of granites determined by high resolution MC-ICP-MS", by F. Poitrasson and R. Freydier [Chem. Geol. 222 132-147]. *Chemical Geology* **235**, 201-204.

Beard, B. L., Johnson, C. M., Skulan, J. L., Nealson, K. H., Cox, L., and Sun, H., 2003a. Application of Fe isotopes to tracing the geochemical and biological cycling of Fe. *Chemical Geology* **195**, 87-117.

Beard, B. L., Johnson, C. M., VonDamm, K. L., and Poulson, R. L., 2003b. Iron isotope constraints on Fe cycling and mass balance in oxygenated Earth oceans. *Geology* **31**, 629-632.

Bennett, S. A., Achterberg, E. P., Connelly, D. P., Statham, P. J., Fones, G. R., and German, C. R., 2008. The distribution and stabilisation of dissolved Fe in deep-sea hydrothermal plumes. *Earth Planet. Sci. Lett.* **270**, 157-167.

Bergquist, B. and Boyle, E., 2006. Iron isotopes in the Amazon river system: weathering and transport signatures. *Earth Planet. Sci. Lett.* **248**, 54-68.

Boyd, P. W., Watson, A. J., Law, C. S., Abraham, E. R., Trull, T., R.Murdoch, Bakker, D. C. E., Bowie, A., Buesseler, K. O., Chang, H., Charette, M., Croot, P., Downing, K., Frew, R., Gall, M., Hadfield, M., Hall, J., Harvey, M., Jameson, G., DeLaRoche, J., Liddicoat, M., Ling, R., Maldonado, M. T., McKay, R. M., Nodder, S., Pickmere, S., Pridmore, R., Rintoul, S., Safi, K., Sutton, P., Strzepek, R., Tanneberger, K., Turner, S., Waite, A., and Zeldis, J., 2000. A mesoscale phytoplankton bloom in the polar Southern Ocean stimulated by iron fertilization. *Nature* **407**, 695-702.

Boyle, E., Collier, R., Dengler, A. T., Edmond, J. M., Ng, A. C., and Stallard, R. F., 1974. On the chemical mass-balance in estuaries. *Geochimica et Cosmochimica Acta* **38**, 1719-1728.

Boyle, E. A., Bergquist, B. A., Kayser, R. A., and Mahowald, N., 2005. Iron, manganese, and lead at Hawaii Ocean Time-series station ALOHA: Temporal variability and an intermediate water hydrothermal plume. *Geochim. Cosmochim. Acta* **69**, 933-952.

Boyle, E. A., Edmond, J. M., and Sholkovitz, E. R., 1977. The mechanism of iron removal in estuaries. *Geochimica et Cosmochimica Acta* **41**, 1313-1324.

Brantley, B. L., Liermann, L. J., Guynn, R. L., Anbar, A., Icopini, G. A., and Barling, J., 2004. Fe isotopic fractionation during mineral dissolution with and without bacteria. *Geochim. Cosmochim. Acta* **68**, 3189-3204.

Brantley, S. L., Liermann, L., and Bullen, T. D., 2001. Fractionation of Fe isotopes by soil microbes and organic acids. *Geology* **29**, 535-538.

Christian, J. R., Verschell, M. A., Murtugudde, R., Busalacchi, A. J., and McClain, C. R., 2002. Biogeochemical modelling of the tropical Pacific Ocean. II: Iron biogeochemistry. *Deep-Sea Res. II* **49**, 545-565.

Gledhill, M. and van den Berg, C. M. G., 1994, Determination of complexation of iron(III) with natural organic complexing ligands in seawater using cathodic stripping voltammetry. *Marine Chemistry* 47(1): 41-54.

Crerar, D. A., Means, J. L., Yuretich, R. F., Borcsik, M. P., Amster, J. L., Hastings, D. W., Knox, G. W., Lyon, K. E., and Quiett, R. F., 1981. Hydrogeochemistry of the New Jersey coastal plain 2. Transport and deposition of iron, alumunium, dissolved organic matter, and selected trace elements in stream, ground- and estuary water. *Chemical Geology* **33**, 23-44.

Dauphas, N. and Rouxel, O., 2006. Mass spectrometry and natural variations of iron isotopes. *Mass Spectrometry Reviews* **25**, 515-550.

de Jong, J., Schoemann, V., Tison, J.-L., Becquevort, S., Masson, F., Lannuzel, D., Petit, J., Choua, L., Weis, D., and Mattielli, N., 2007. Precise measurement of Fe isotopes in marine samples by multi-collector inductively coupled plasma mass spectrometry (MC-ICP-MS). *Analytica Chimica Acta* **589**, 105-119.

Dideriksen, K., Baker, J. A., and Stipp, S. L. S., 2008. Equilibrium Fe isotope fractionation between inorganic aqueous Fe(III) and the siderophore complex, Fe(III)-desferrioxamine B. *Earth and Planetary Science Letters* **269**, 280-290.

Eckert, J. and Sholkovitz, E. R., 1976. The flocculation of iron, aluminum and humates from river water by electrolytes. *Geochimica et Cosmochimica Acta* **40**, 847-848.

Elderfield, H. and Schultz, A., 1996. Mid-ocean ridge hydrothermal fluxes and the chemical composition of the ocean. *Annu. Rev. Earth Planet. Sci.* **24**, 191-224.

Elrod, V. A., Berelson, W. M., Coale, K. H., and Johnson, K. S., 2004. The flux of iron from continental shelf sediments: A missing source for global budgets. *Gephysical Research Letters* **31**, doi:10.1029/2004GL020216.

Fantle, M. S. and DePaolo, D. J., 2004. Iron isotopic fractionation during continental weathering. *Earth Planet. Sci. Lett.* **228**, 547-562.

Forsgren, G., Jansson, M., and Nilsson, P., 1996. Aggregation and Sedimentation of Iron, Phosphorus and Organic Carbon in Experimental Mixtures of Freshwater and Estuarine Water. *Estuarine, Coastal and Shelf Science* **43**, 259-268.

Fox, L. E. and Wofsy, S. C., 1983. Kinetics of removal of iron colloids from estuaries. *Geochimica et Cosmochimica Acta* **47**, 211-216.

Garvine, R. W., 1975. The distribution of salinity and temperature in the Connecticut River Estuary. *Journal of Geophysical Research* **80**, 1176-1183.

Guelke, M. and vonBlanckenburg, F., 2007. Fractionation of Stable Iron Isotopes in Higher Plants. *Environ. Sci. Technol.* **41**, 1896-1901.

Gustafsson, O., Widerlund, A., Andersson, P. S., Ingri, J., Ross, P., and Ledin, A., 2000. Colloid dynamics and transport of major elements through a boreal river - brackish bay mixing zone. *Mar. Chem.* **71**, 1-21.

Huh, Y., Chan L.-H., and Edmond J., 2001. Lithium isotopes as a probe of weathering processes: Orinoco River. *Earth and Planetary Science Letters* 194(1-2): 189-199.

750 Hunter, K. A., 1990. Kinetics and mechanisms of iron colloid aggregation in estuaries. In:
751 Beckett, R. (Ed.), *Surface and Colloid Chemistry in Natural Waters and Water*
752 *Treatment*. Plenum Press, New York.
753 Hunter, K. A., Leonard, M. R., Carpenter, P. D., and Smith, J. D., 1997. Aggregation of
754 iron colloids in estuaries: a heterogeneous kinetics study using continuous mixing
755 of river and sea waters. *Colloids and Surfaces A: Physicochemical and*
756 *Engineering Aspects* **120**, 111-121.
757 Hydes, D. J. and Liss, P. S., 1977. The behavior of dissolved aluminum in estuarine and
758 coastal waters. *Estuarine and Coastal Marine Science* **5**, 755-769.
759 Icopini, G. A., Anbar, A. D., Ruebush, S. S., Tien, M., and Brantley, S. L., 2004. Iron
760 isotope fractionation during microbial reduction of iron: The importance of
761 adsorption. *Geology* **32**, 205-208.
762 Ingri, J., Malinovsky, D., Rodushkin, I., Baxter, D. C., Widerlund, A., Andersson, P.,
763 Gustafsson, Ö., Forsling, W., and Öhlander, B., 2006. Iron isotope fractionation in
764 river colloidal matter. *Earth and Planetary Science Letters* **245**, 792-798.
765 Jickells, T. D., An, Z. S., Andersen, K. K., Baker, A. R., Bergametti, G., Brooks, N., Cao,
766 J. J., Boyd, P. W., Duce, R. A., Hunter, K. A., Kawahata, H., Kubilay, N.,
767 laRoche, J., Liss, P. S., Mahowald, N., Prospero, J. M., Ridgwell, A. J., Tegen, I.,
768 and Torres, R., 2005. Global Iron Connections Between Desert Dust, Ocean
769 Biogeochemistry, and Climate. *Science* **308**, 67-71.
770 Johnson, C. M. and Beard, B. L., 2006. Fe isotopes: an emerging technique in
771 understanding modern and ancient biogeochemical cycles. *GSA Today* **16**, 4-10.
772 Johnson, C. M., Beard, B. L., Roden, E. E., Newman, D. K., and Nealson, K. H., 2004.
773 Isotopic constraints on biological cycling of Fe. *Reviews in Mineralogy and*
774 *Geochemistry* **55**, 359-408.
775 Johnson, K. S., Chavez, F. P., and Friederich, G. E., 1999. Continental-shelf sediment as a
776 primary source of iron for coastal phytoplankton. *Nature* **398**, 697-700.
777 Johnson, K. S., Gordon, R. M., and Coale, K. H., 1997. What controls dissolved iron
778 concentrations in the world ocean ? *Marine Chemistry* **57**, 137-161.
779 Lefevre, N. and Watson, A. J., 1999. Modeling the geochemical cycle of iron in the
780 oceans and its impact on atmospheric CO2 concentrations. *Global Biogeochemical*
781 *Cycles* **13**, 727-736.
782 Martin, J. H., 1990. Glacial-interglacial CO2 change: the iron hypothesis.
783 *Paleoceanography* **5**, 1-13.
784 Mayer, L. M., 1982. Retention of riverine iron in estuaries. *Geochim. Cosmochim. Acta*
785 **46**, 1003-1009.
786 Moore, J. K., Doney, S. C., Glover, D. M., and Fung, I. Y., 2002. Iron cycling and
787 nutrient-limitation patterns in surface waters of the World Ocean. *Deep-Sea Res. II*
788 **463-507**.
789 Moore, J. K., Doney, S. C., and Lindsay, K., 2004. Upper ocean ecosystem dynamics and
790 iron cycling in a global 3-D model. *Global Biogeochem. Cycles* **18**,
791 doi:10.1029/2004GB002220.
792 Plank, T. and Langmuir, C. H., 1998. The chemical composition of subducting sediment
793 and its consequences for the crust and mantle. *Chemical Geology* **145**, 325-394.
794 Poitrasson, F., 2006. On the iron isotope homogeneity level of the continental crust.
795 *Chemical Geology* **235**, 195-200.
796 Poitrasson, F. and Freydier, R., 2005. Heavy iron isotope composition of granites
797 determined by high resolution MC-ICP-MS. *Chemical Geology* **222**, 132-147.
798 Poulton, S. W. and Raiswell, R., 2002. The low-temperature geochemical cycle of iron:
799 from continental fluxes to marine sediment deposition. *Am. J. Sci.* **302**, 774-805.

800 Ross, J. M. and Sherrell, R. M., 1999. The role of colloids in trace metal transport and
801 adsorption behavior in New Jersey Pinelands streams. *Limnol. Oceanogr.* **44**,
802 1019-1034.
803 Rouxel, O., N. Dobbek, Ludden, J. and Fouquet, Y. 2003, Iron isotope fractionation
804 during oceanic crust alteration. *Chemical Geology* 202(1-2): 155-182.
805 Rouxel, O., Bekker, A., and Edwards, K., 2005. Iron Isotope Constraints on the Archean
806 and Paleoproterozoic Ocean Redox State. *Science* **307**, 1088-1091.
807 Rouxel, O., Shanks, W. C., Bach, W., and Edwards, K., 2008a. Integrated Fe and S
808 isotope study of seafloor hydrothermal vents at East Pacific Rise 9-10N. *Chem.*
809 *Geol.* **252**, 214-227.
810 Rouxel, O., Sholkovitz, E., Charette, M., and Edwards, K., 2008b. Iron Isotope
811 Fractionation in Subterranean Estuaries. *Geochem. Cosmochim. Acta* **72**, 3413-
812 3430.
813 Rouxel, O. Natural variations of Fe isotopic compositions of seawater determined by MC-
814 ICPMS. 2009. *Geophysical Research Abstracts,* 11, EGU2009-10517.
815 Rudnick, R. L. and Gao, S., 2007. Composition of the Continental Crust. *Treatise on*
816 *Geochemistry* Chapter 3.01, 1-64.
817 Schauble, E.A., 2004. Applying stable isotope fractionation theory to new systems. In:
818 Johnson, C.M., Beard, B.L., Albarede, F. (Eds.), Geochemistry of Non-traditional
819 Stable Isotopes. *Mineralogical Society of America*, Washington DC, pp. 65–111.
820 Severmann, S., Johnson, C. M., Beard, B. L., and McManus, J., 2006. The effect of early
821 diagenesis on the Fe isotope compositions of porewaters and authigenic minerals
822 in continental margin sediments. *Geochimica et Cosmochimica Acta* **70**, 2006-
823 2022.
824 Severmann, S., Lyons, T. W., Anbar, A., McManus, J., and Gordon, G., 2008. Modern
825 iron isotope perspective on the benthic iron shuttle and the redox evolution of
826 ancient oceans. *Geology* **36**, 487-490.
827 Sholkovitz, E. R., 1976. Flocculation of dissolved organic and inorganic matter during the
828 mixing of river water and seawater. *Geochimica et Cosmochimica Acta* **40**, 831-
829 845.
830 Sholkovitz, E. R., 1978. The flocculation of dissolved Fe, Mn, Al, Cu, Ni, Co and Cd
831 during estuarine mixing. *Earth and Planetary Science Letters* **41**, 77-86.
832 Sholkovitz, E. R., Boyle, E. A., and Price, N. B., 1978. The removal of dissolved humic
833 acids and iron during estuarine mixing. *Earth and Planetary Science Letters* **40**,
834 130-136.
835 Skulan, J. L., Beard, B. L., and Johnson, C. M., 2002. Kinetic and equilibrium Fe isotope
836 fractionation between aqueous Fe(III) and hematite. *Geochimica et Cosmochimica*
837 *Acta* **66**, 2995-3015.
838 Staubwasser, M., von Blanckenburg, F., and Schoenberg, R., 2006. Iron isotopes in the
839 early marine diagenetic iron cycle. *Geology*, **34**, 629–632.
840 Stookey, L. L., 1970. FerroZine– a new spectrophotometric reagent for iron. *Anal. Chem.*
841 **42**, 779-781.
842 Taylor, S. R., McLennan, S. M., and McCulloch, M. T., 1983. Geochemistry of loess,
843 continental crustal composition and crustal model ages. *Geochimica et*
844 *Cosmochimica Acta* **47**, 1897-1905.
845 Teutsch, N., vonGunten, U., Porcelli, D., Cirpka, O. A., and Halliday, A. N., 2005.
846 Adsorption as a cause for Iron Isotope fractionation in reduced groundwater.
847 *Geochim. Cosmochim. Acta* **17**, 4175-4185.

Thompson, A., Ruiz, J., Chadwick, O. A., Titus, M., and Chorover, J., 2007. Rayleigh fractionation of iron isotopes during pedogenesis along a climate sequence of Hawaiian basalt. *Chemical Geology* **238**, 72-83.

Upadhyay, S., 2008. Sorption model for dissolved and particulate aluminium in the Conway estuary, UK. *Estuarine and Coastal Marine Science* **76**, 914-919.

Urey, C.H., 1947. The thermodynamic properties of isotopic substances. *J. Chem. Soc*. 562–581.

Van den Berg, C. M. G., 1995, Evidence for organic complexation of iron in seawater. *Marine Chemistry* 50(1-4): 139-157.

Wedepohl, K. H., 1995. The composition of the continental crust. *Geochimica et Cosmochimica Acta* **59**, 1217-1232.

Wells, M. L., Price, N. M., and Bruland, K. W., 1995. Iron chemistry in seawater and its relationship to phytoplankton: a workshop report. *Marine Chemistry* **48**, 157-182.

Weyer, S. and Schwieters, J. B., 2003. High precision Fe isotope measurements with high mass resolution MC-ICPMS. *International Journal of Mass Spectrometry* **226**, 355-368.

Wiederhold, J. G., Teutsch, N., Kraemer, S. M., Halliday, A. N., and Kretzschmar, R., 2007. Iron isotope fractionation in oxic soils by mineral weathering and podzolization. *Geochimica et Cosmochimica Acta* **71**, 5821-5833.

Wu, J., Boyle, E., Sunda, W., and Wen, L.-S., 2001. Soluble and colloidal iron in the Oligotrophic North Atlantic and North Pacific. *Science* **293**, 847-849.

Yan, L., Stallard, R. F., Key, R. M., and Crerar, D. A., 1990. The chemical behavior of trace metals and 226Ra during estuarine mixing in the Mullica River estuary, New Jersey, U.S.A.: A comparison between field observation and equilibrium calculation. *Chemical Geology* **85**, 369-381.

Zhuang, G., Yi, Z., and Wallace, G. T., 1995. Iron(II) in rainwater, snow, and surface seawater from a coastal environment. *Marine Chemistry* **50**, 41-50.

FIGURE CAPTIONS

Figure 1: Map of the North River estuary showing sampling sites at low and high tides. Sample name are also shown for each sampling site.

Figure 2: Color and concentrations of Fe, Al, Mo, Mn (μM) and Ca (mM) of the dissolved fraction (<0.22 μm) versus salinity along the North River estuary. Sampling during ebb (open diamonds) and flood (gray diamonds) tides are shown for comparison.

Figure 3: Concentrations of particulate Fe (>0.22 μm) and dissolved versus particulate Fe ratios along the salinity profile. Sampling during ebb and flood tides are shown in open and gray diamonds respectively.

Figure 4: Fraction of Fe removed (i.e. flocculation factor F) along the North River estuary. Fe concentrations *vs.* salinity are shown for comparison.

Figure 5: Fe-isotope compositions of dissolved Fe (<0.22 μm) and particulate Fe (>0.22 μm) along the salinity gradient. Horizontal gray bar corresponds to average δ^{56}Fe values for crustal rocks (Beard et al., 2001; Dauphas and Rouxel, 2006).

Figure 6: Al/Fe ratios of dissolved Fe (<0.22 μm) and particulate Fe (>0.22 μm) along the salinity gradient at North River estuary.

Figure 7: Iron isotope composition of dissolved pool *versus* the fraction (F) of Fe removed through flocculation process. A) a linear relationship between δ^{56}Fe and 1/(1-F) is expected if truly dissolved Fe in rivers is different from riverine colloids; B) a linear relationship between δ^{56}Fe and –log(1-F) is expected if colloid flocculation process produce significant Fe-isotope fractionation between coagulated colloids and remaining dissolved colloids.

Figure 8: (A) δ^{56}Fe *vs.* Al/Fe ratios of dissolved Fe (<0.22 μm) and particulate Fe (>0.22 μm) at North River estuary showing a 3-component mixing relationship between (1) riverine colloids (X_{col}) (2) river borne particles (X_{RP}) and (3) lithogenic particles (X_{Litho})

910 from high salinity end-members. (B) Variations of X_{col} , X_{RP} and X_{Litho} with salinity. See
911 text for discussion.
912
913 Figure 9: Relationship between the X_{Col}/X_{RP} and the fraction (F) of Fe removed through
914 flocculation. X_{Col} and X_{RP} represent the fractions of particulate Fe from coagulated
915 colloids and river borne particles respectively. As expected, the ratio X_{Col}/X_{RP} increase
916 linearly with F along a 1:1 slope reflecting the addition of particles along the estuary due
917 to flocculation process. This relationship also suggests a minimal loss of particulate Fe
918 during estuarine mixing.
919
920

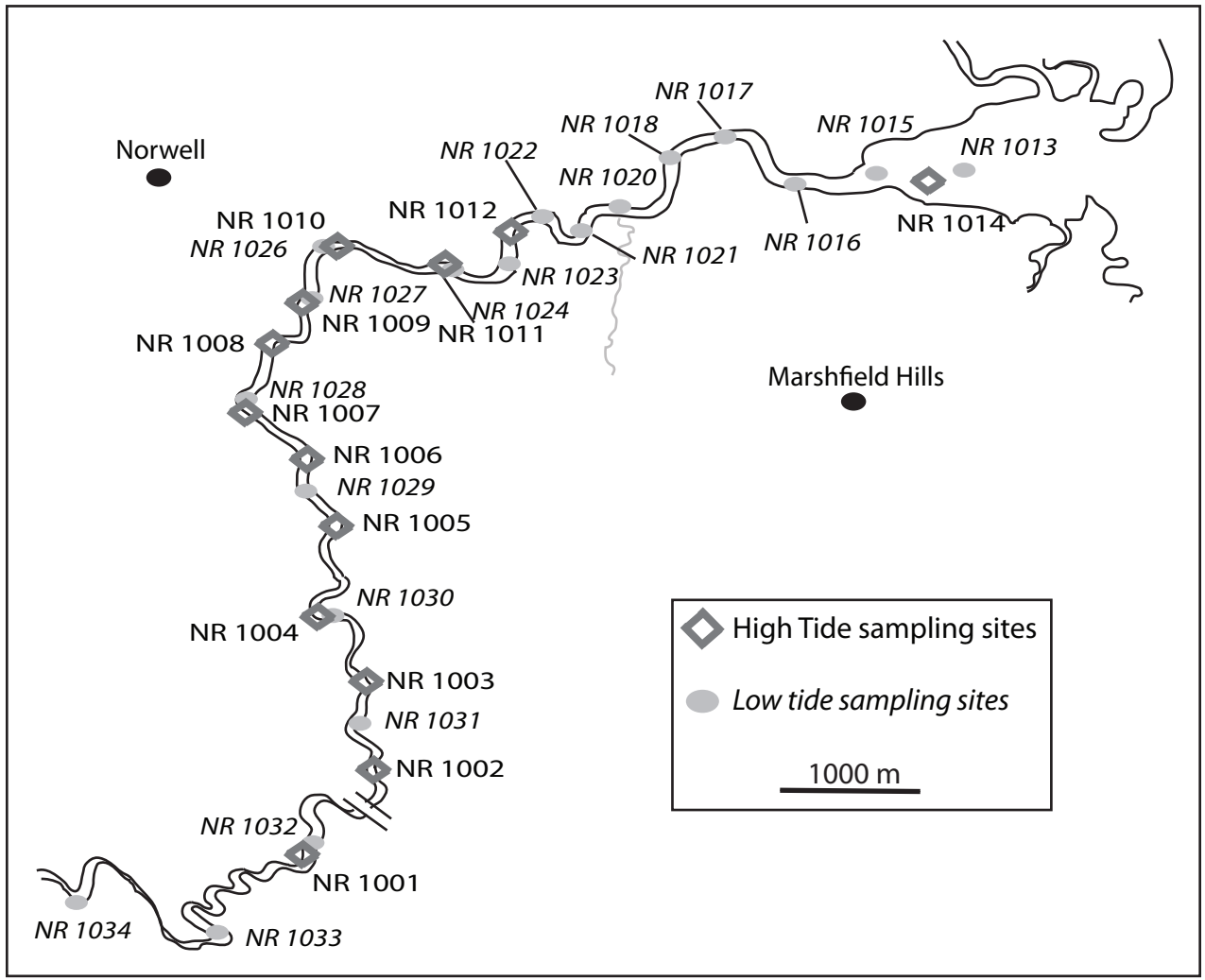
NR 1017
NR 1018
NR 1015
NR 1013
Norwell
NR 1022
NR 1020
NR 1012
NR 1010
NR 1026
NR 1016
NR 1014
NR 1021
NR 1023
NR 1027
NR 1024
NR 1009
NR 1008
NR 1011
Marshfield Hills
NR 1028
NR 1007
NR 1006
NR 1029
NR 1005
NR 1030
NR 1004
NR 1003
NR 1031
NR 1002
NR 1032
NR 1001
NR 1034
NR 1033
High Tide sampling sites
Low tide sampling sites
1000 m

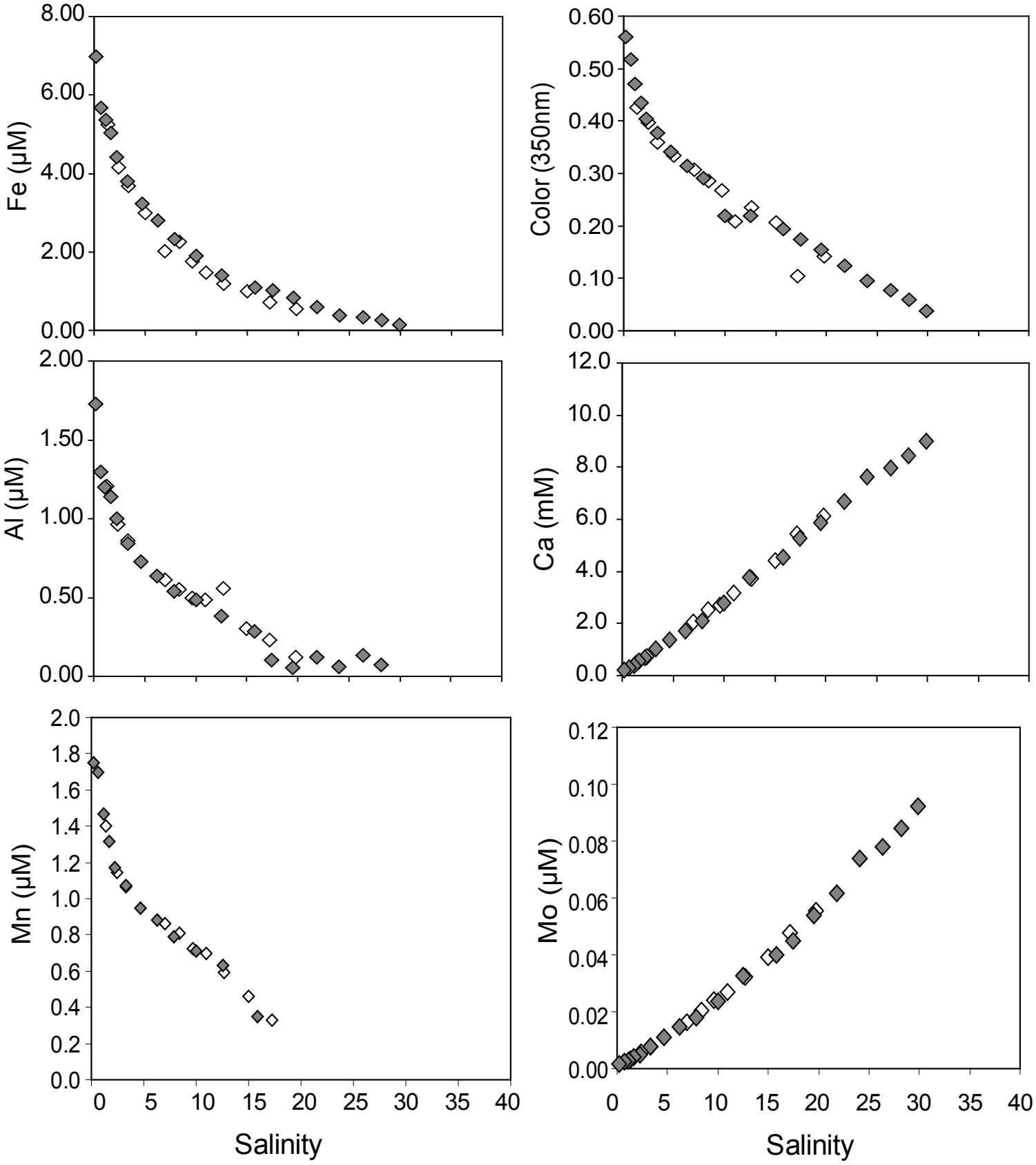

Figure 2

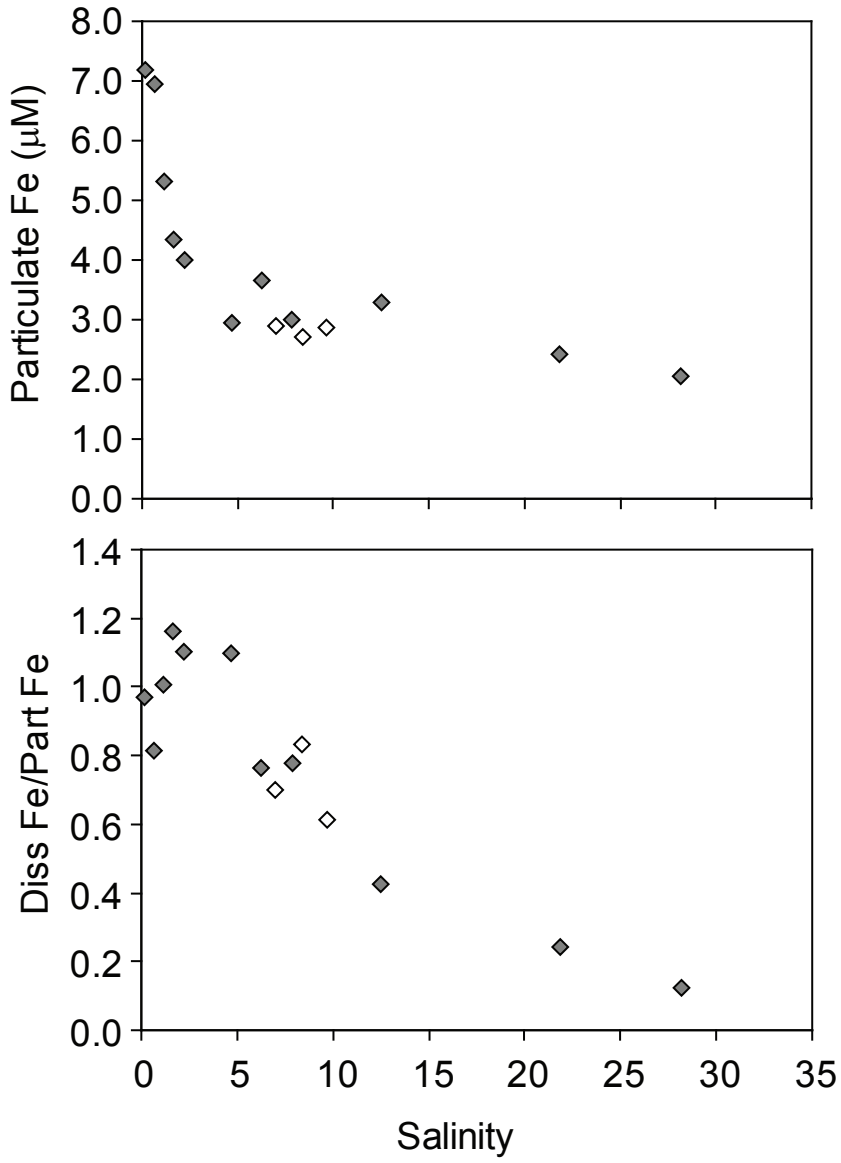
Particulate Fe (µM)
8.0
7.0
6.0
5.0
4.0
3.0
2.0
1.0
0.0
Diss Fe/Part Fe
1.4
1.2
1.0
0.8
0.6
0.4
0.2
0.0
0
5
10
15
20
25
30
35
Salinity

Figure 3

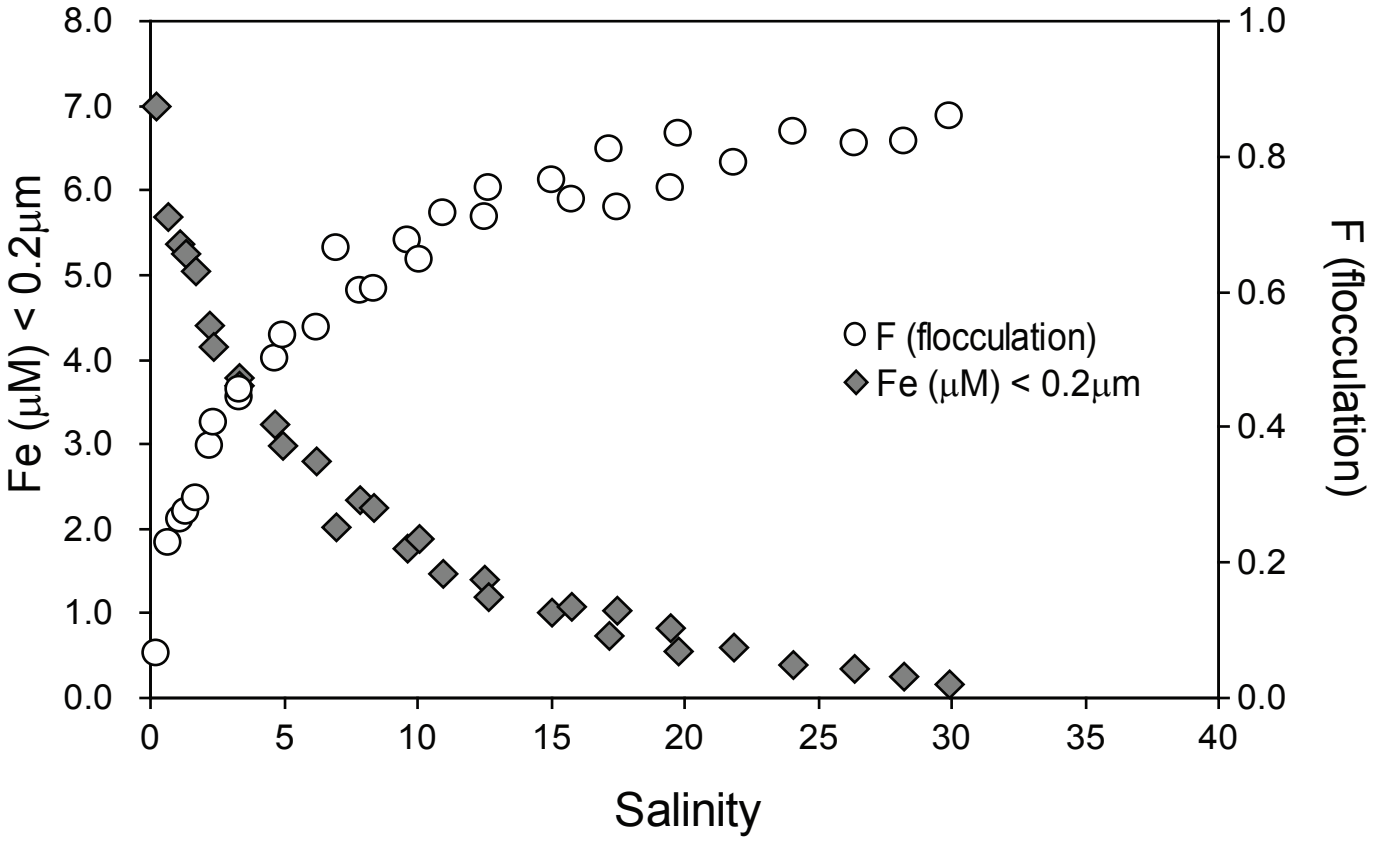
8.0
7.0
6.0
5.0
4.0
3.0
2.0
1.0
0.0
Fe (μM) < 0.2μm
1.0
0.8
0.6
0.4
0.2
0.0
F (flocculation)
0
5
10
15
20
25
30
35
40
Salinity
F (flocculation)
Fe (μM) < 0.2μm

Figure 4

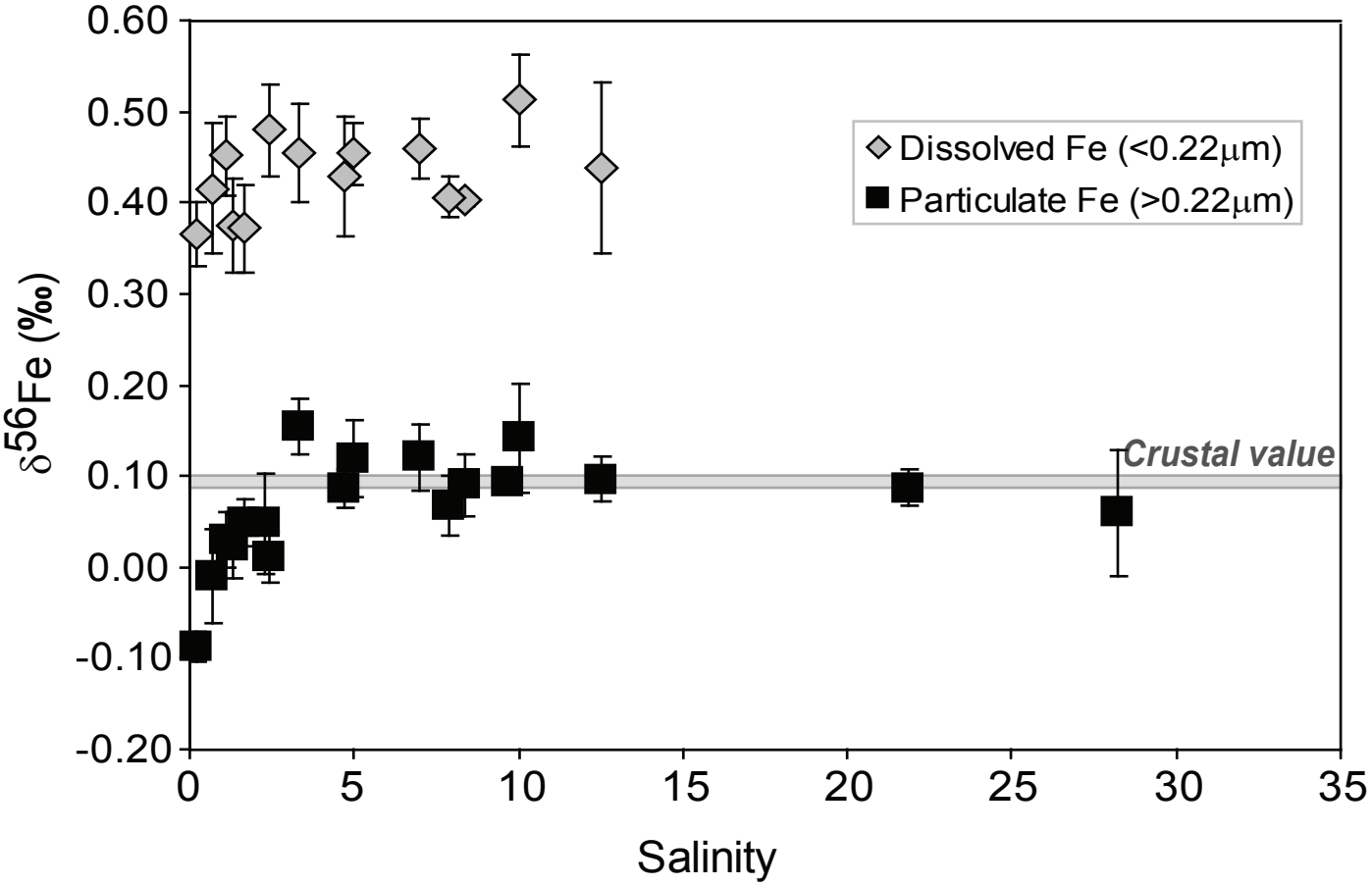
0.60
0.50
0.40
0.30
0.20
0.10
0.00
-0.10
-0.20
δ56Fe (‰)
0
5
10
15
20
25
30
35
Salinity
Dissolved Fe (<0.22μm)
Particulate Fe (>0.22μm)
Crustal value

Figure 5

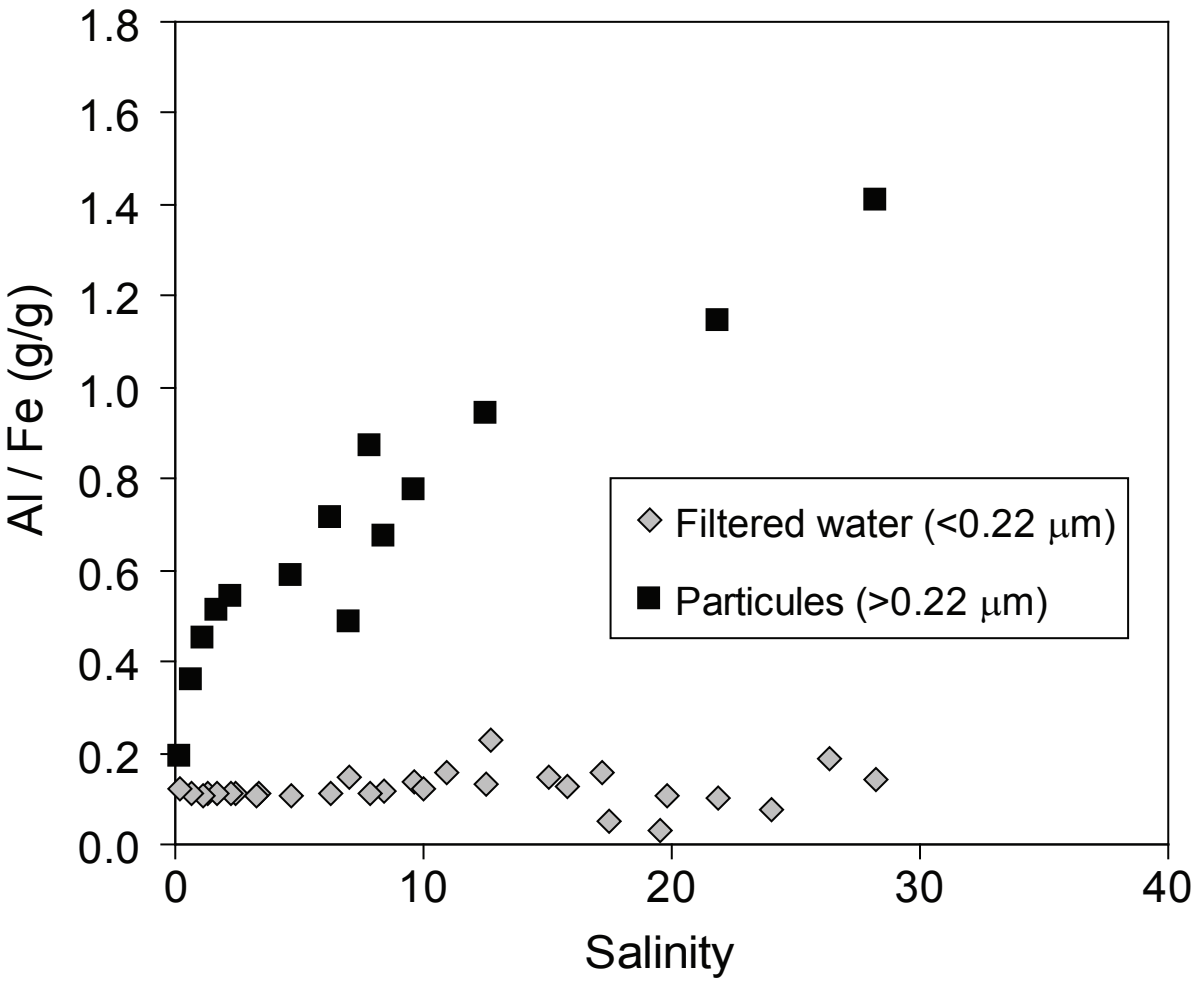
1.8
1.6
1.4
1.2
1.0
0.8
0.6
0.4
0.2
0.0
Al / Fe (g/g)
0
10
20
30
40
Salinity
Filtered water (<0.22 μm)
Particules (>0.22 μm)

Figure 6

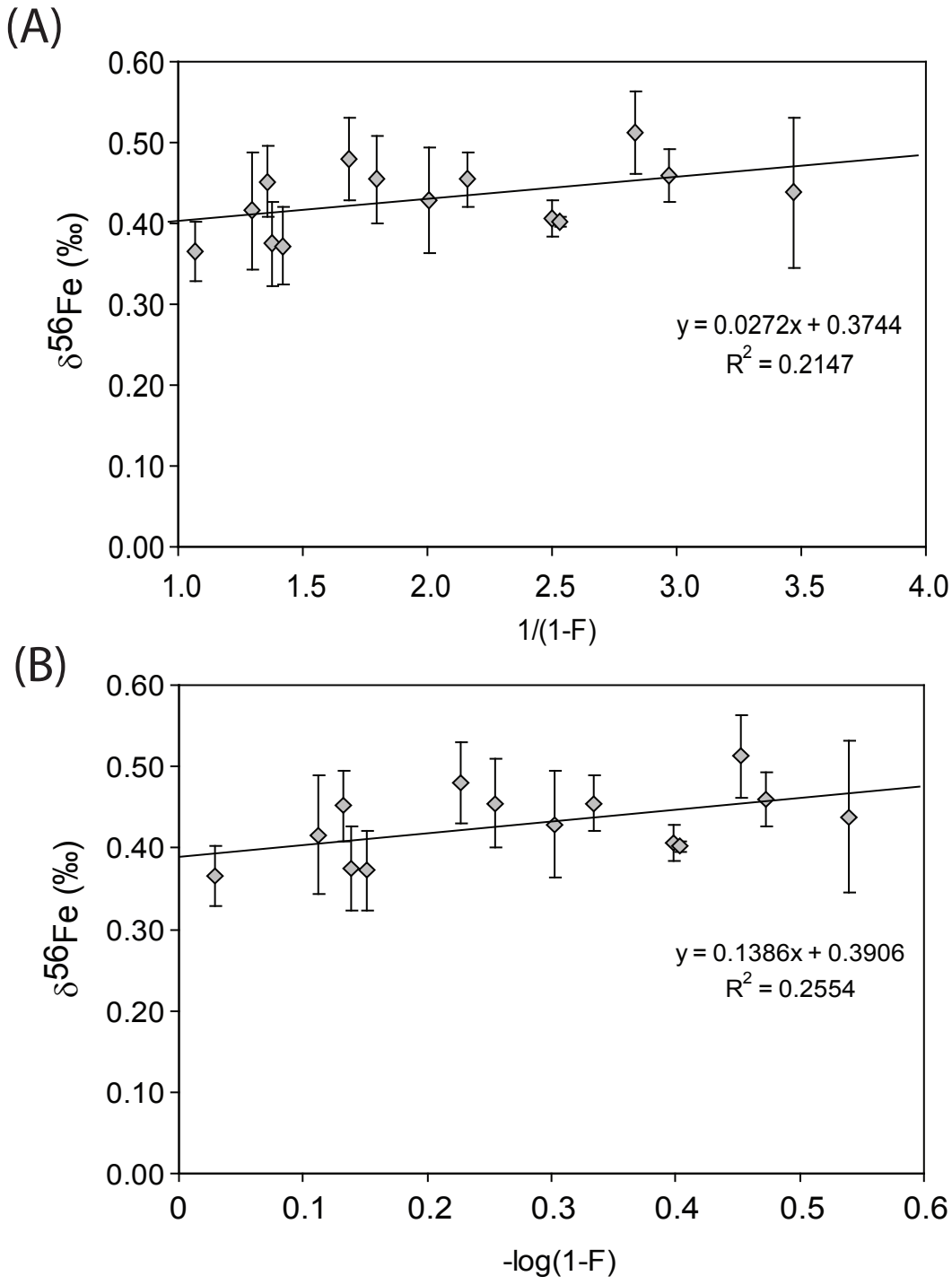
(A)
0.60
0.50
0.40
0.30
0.20
0.10
0.00
δ56Fe (‰)
y = 0.0272x + 0.3744
R2 = 0.2147
1.0
1.5
2.0
2.5
3.0
3.5
4.0
1/(1-F)
(B)
0.60
0.50
0.40
0.30
0.20
0.10
0.00
δ56Fe (‰)
y = 0.1386x + 0.3906
R2 = 0.2554
0
0.1
0.2
0.3
0.4
0.5
0.6
-log(1-F)

Figure 7

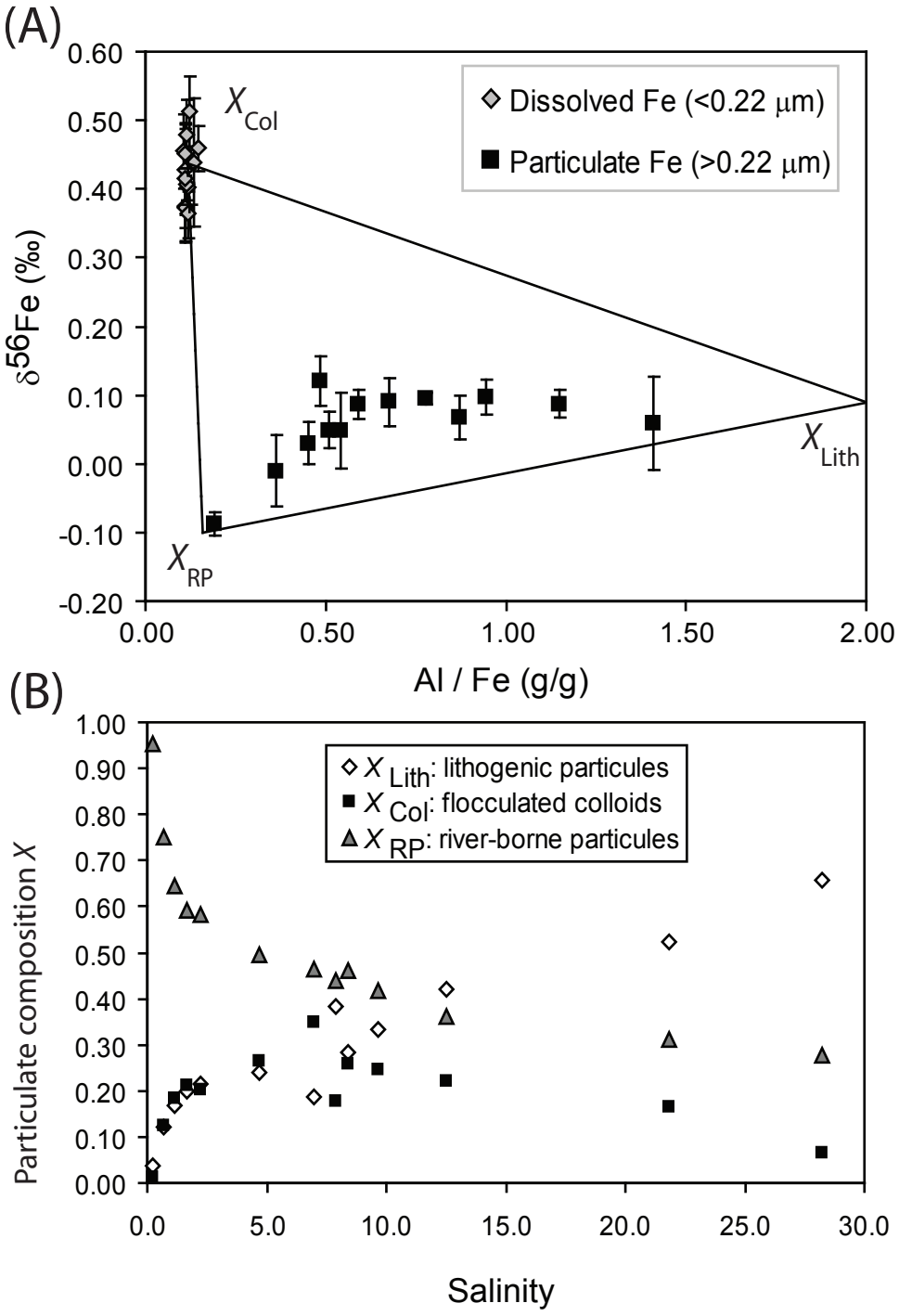
(A)
Dissolved Fe (<0.22 μm)
Particulate Fe (>0.22 μm)
X_{Col}
X_{Lith}
X_{RP}
δ^{56}Fe (‰)
Al / Fe (g/g)
(B)
X_{Lith}: lithogenic particules
X_{Col}: flocculated colloids
X_{RP}: river-borne particules
Particulate composition X
Salinity

Figure 8

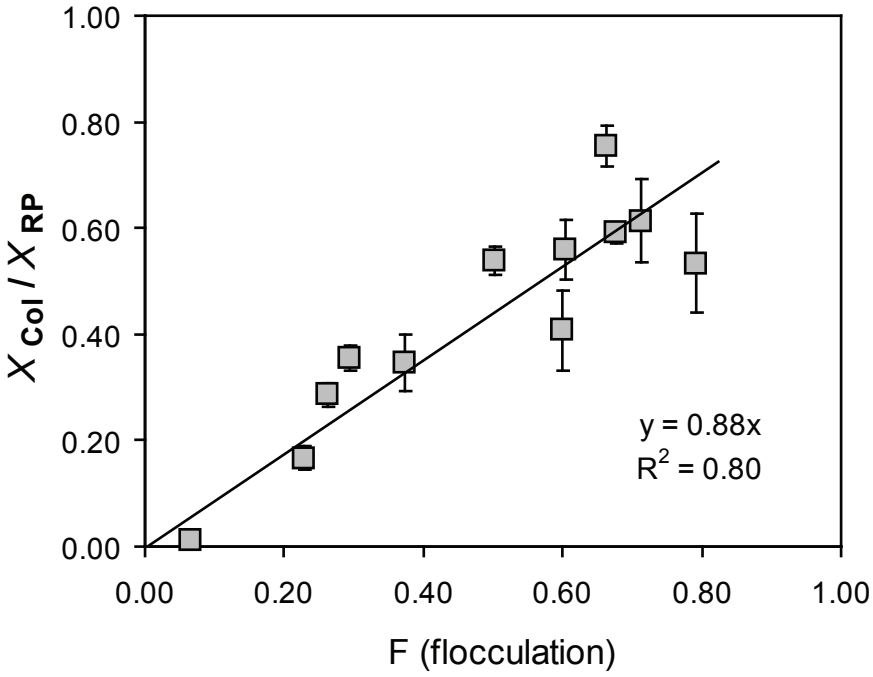
1.00
0.80
0.60
0.40
0.20
0.00
0.00
0.20
0.40
0.60
0.80
1.00
X Col / X RP
F (flocculation)
y = 0.88x
R2 = 0.80

Figure 9

Table 1: Chemical and isotopic composition of filtered North River estuary samples

Sample Name	Salinity	color at 350 nm	Fe (μM)	Al (μM)	Ca (mM)	Mo (μM)	Mn (μM)	N#	δ^{56}Fe	1σ	δ^{57}Fe	1σ
ebb tide												
NR-1001	1.33	0.426	5.24	1.21	0.5	0.003	1.40	5	0.37	0.05	0.56	0.09
NR-1002	2.40	0.397	4.15	0.96	0.7	0.006	1.14	6	0.48	0.05	0.69	0.08
NR-1004	4.99	0.334	2.98	-	-	-	-	4	0.45	0.03	0.70	0.04
NR-1005	6.97	0.307	2.02	0.62	2.0	0.016	0.86	5	0.46	0.03	0.65	0.08
NR-1006	8.40	0.286	2.25	0.55	2.5	0.020	0.81	2	0.40	0.01	0.57	0.08
flood tide												
NR-1021	12.51	0.22	1.39	0.38	3.8	0.033	0.63	2	0.44	0.09	0.66	0.12
NR-1022	10.04	0.219	1.89	0.48	2.8	0.023	0.71	2	0.51	0.05	0.78	0.08
NR-1023	7.86	0.291	2.33	0.54	2.1	0.018	0.79	6	0.41	0.02	0.61	0.06
NR-1025	4.67	0.341	3.24	0.73	1.4	0.011	0.95	5	0.43	0.07	0.64	0.06
NR-1026	3.31	0.377	3.79	0.84	1.0	0.008	1.07	12	0.45	0.05	0.67	0.07
NR-1028	1.68	0.435	5.04	1.14	0.5	0.004	1.32	6	0.37	0.05	0.57	0.06
NR-1029	1.12	0.471	5.36	1.20	0.4	0.003	1.47	5	0.45	0.04	0.68	0.07
NR-1030	0.69	0.518	5.68	1.29	0.3	0.002	1.70	6	0.42	0.07	0.59	0.05
NR-1033	0.20	0.56	6.98	1.73	0.2	0.002	1.75	6	0.37	0.04	0.55	0.06

#: number of duplicated Fe-isotope analysis

- : not determined

Table2: Chemical and Fe-isotope composition of suspended particles in North River estuary

Sample Name	Salinity	Al (μM)	Fe (μM)	Ti (μM)	Ca (μM)	Mn (μM)	N#	δ^{56}Fe	1σ	δ^{57}Fe	1σ
NR 1001 F	1.33	-	-	-	-	-	7	0.02	0.04	0.06	0.04
NR 1002 F	2.40	-	-	-	-	-	8	0.01	0.03	0.11	0.04
NR 1004 F	4.99	-	-	-	-	-	8	0.12	0.04	0.18	0.03
NR 1005 F	6.97	2.92	2.90	0.08	2.49	0.07	8	0.12	0.04	0.23	0.06
NR 1006 F	8.4	3.79	2.71	0.10	2.80	0.06	13	0.09	0.03	0.16	0.07
NR 1007 F	9.66	4.61	2.87	0.12	3.28	0.07	5	0.09	0.01	0.17	0.02
NR 1014 F	28.2	5.98	2.05	0.17	7.88	0.04	4	0.06	0.07	0.12	0.04
NR 1017 F	21.84	5.75	2.42	0.16	6.55	0.04	7	0.09	0.02	0.11	0.06
NR 1021 F	12.51	6.42	3.29	0.19	4.56	0.07	8	0.10	0.02	0.14	0.06
NR 1022 F	10.04	-	-	-	-	-	7	0.14	0.06	0.28	0.07
NR 1023 F	7.86	5.40	3.00	0.15	3.25	0.08	10	0.07	0.03	0.11	0.06
NR 1024 F	6.25	5.43	3.66	0.17	2.93	0.09		-		-	
NR 1025 F	4.67	3.60	2.95	0.09	2.21	0.06	8	0.09	0.02	0.09	0.03
NR 1026 F	3.31	-	-	-	-	-	4	0.15	0.03	0.24	0.03
NR 1027 F	2.25	4.48	4.00	0.12	1.84	0.10	7	0.05	0.05	0.09	0.08
NR 1028 F	1.68	4.57	4.33	0.11	1.74	0.11	5	0.05	0.03	0.10	0.03
NR 1029 F	1.12	4.99	5.32	0.13	1.88	0.14	11	0.03	0.03	0.07	0.04
NR 1030 F	0.69	5.20	6.96	0.13	2.26	0.16	12	-0.01	0.05	0.00	0.08
NR 1033 F	0.2	2.85	7.19	0.07	3.04	0.15	6	-0.09	0.02	-0.11	0.04

#: number of duplicated Fe-isotope analysis

- : not determined

Table 3: Fe concentration and isotope composition of North River for different filter size

	Size fraction (μm)	[Fe] μM	N#	δ^{56}Fe	1σ	δ^{57}Fe	1σ
Water							
NR II E*	< 0.22*	8.65	6	0.34	0.03	0.55	0.08
NR II A	< 0.22	8.76	6	0.38	0.02	0.55	0.02
NR II B	< 0.1	*8.6***	14	0.38	0.06	0.54	0.08
NR II C	< 0.05	*8.2***	6	0.44	0.03	0.65	0.03
NR II D	< 0.025	*8.6***	5	0.42	0.02	0.58	0.03
Particules							
NR II A F	>0.22	3.17	6	-0.22	0.01	-0.32	0.07
NR II B F	0.22 - 0.1	0.08	3	-0.12	0.04	-0.22	0.03
NR II C F	0.22 - 0.05	0.47	9	0.14	0.02	0.21	0.03
NR II D F	0.22 - 0.025	0.07	3	0.09	0.08	0.24	0.10

* filtration through 0.22um Millipak™ cartridge instead of Durapore™ 45mm membrane

** calculated by mass balance using particulate Fe concentration

#: number of duplicated Fe-isotope analysis

Table 4: Fe-isotope composition and percent of Fe removal in North River and other east coast estuaries

Estuary	Date	River water end-member Fe (μM)	δ^{56}Fe river end-member	(1σ)	Zero-salinity intercept Fe (μM)	% removal	Reference
Connecticut	07/1973	8.5	-		2.5	71	Boyle et al., 1977
	11/1973	3.1	-		0.9	71	Boyle et al., 1977
	11/2006	1.4	**0.18**	0.03	-	-	This study
	05/2007	1.3	-		0.5	64	This study
Merrimack	07/1973	4.0	-		1.5	63	Boyle et al., 1977
	08/1973	3.5	-		1.0	71	Boyle et al., 1977
	10/1973	3.7	-		1.7	54	Boyle et al., 1977
Mullica	09/1973	23.4	-		1.0	96	Boyle et al., 1977
	06/2007	8.3	**-0.33**	0.02	-	-	This study
North River	05/2006	8.9	**0.14**	0.05	3.3	63	This study
	10/2006	7.5	**0.37**	0.04	1.4	82	This study
	11/2006	8.6	**0.34**	0.03	n.d.	n.d.	This study

- : not determined